



Egyptian Journal of Chemistry



Indexed in Scopus



Vol. No

Online ISSN: 2357-0245

Print ISSN : 0449-2285

Edited by : The Egyptian Chemical Society

Published by : Academy of Scientific Research and Technology

Informatics Sector and Scientific Services

National Information and Documentation Centre (NIDOC)

Editorial Board



Editor-in-Chief

👤 Mohamed Refaat Mahran

Organic Chemistry

📍 *National Research Centre*

✉ mrh_mahran@yahoo.com

📞 01111273794



Co-Editor-in-Chief

👤 Said Fatouh Hamed

Oils and Fats

📍 *National Research Center*

✉ saidfatouhhamed123@gmail.com

📞 01021489155



👤 Hassan Abdel-Gawad Hassan

Organic Chemistry

📍 *National Research Center*

✉ abdelgawadhassan@hotmail.com

📞 01063157828



👤 Morsy Ahmed El-Asasery

Textile Chemistry

📍 *Synthetic Organic Chemistry*

Dyeing, Printing and Textile Auxiliaries Department, NRC.

✉ elapaserym@yahoo.com

📞 01007894172



👤 Ewies Fawzy Ewies

Organic Chemistry

📍 *Synthetic Organic Chemistry*

Organometallic and organometalloid Chemistry Department, NRC.

✉ ef.ewies@nrc.sci.eg

📞 01009957717



Editor

👤 Elmorsy Khaled

Analytical Chemistry

📍 *National Research Center*

✉ elmorsykhaled@yahoo.com



Ing. Milan Sýs

Analytical Chemistry

📍 Faculty of Chemical Technology – University of Pardubice – Czech Republic

✉ milan.sys@upce.cz



Wael Ibrahim Mortada

Analytical Chemistry

📍 Mansoura University

✉ w.mortada@mans.edu.eg



Shaymaa Abdalla Ismail

Microbial Chemistry

📍 National Research Center

✉ shaymaaabdallaismail@gmail.com



Sahar Awad Allah Hussein

Natural Products

📍 National Research Center

✉ drsahar90@yahoo.com



Hanan Sayed Ibrahim

Environmental Chemistry

📍 National Research Center

✉ drhanansibrahim@gmail.com



Galal A. M. Nawwar

Environmental Chemistry

📍 National Research Center

✉ gnawwar@yahoo.com



Francis Verpoort

Inorganic Chemistry

📍 National Distinguished Expert (China)

Distinguished Fellow IETI (Hong Kong)

Ghent University (Belgium)

Wuhan University of Technology (China)

✉ francis.verpoort@ghent.ac.kr

☎ 0000-0002-5184-5500





Ammar Labib

Inorganic Chemistry

National Research Center
ammaral33@gmail.com



Peter Hesemann

Ionic Liquids and catalysts

Institut Charles Gerhardt Montpellier
UMR 5253 CNRS-UM-ENSCM
Université de Montpellier, Place E. Bataillon, Bât 17, cc 1701
34095 Montpellier cedex 5 - France
<http://Scopus Author ID: 6603113289>
peter.hesemann@univ-montp2.fr
0000-0001-5266-979



Mohamed Othman

Catalysis

NormandieUniv, UNILEHAVRE, CNRS 3038, URCOM, 76600 Le Havre, France
mohamed.othman@univ-lehavre.fr



Ahmed Kamel El-Ziaty

Catalysis

Ain-Shams University
ahm512@sci.asu.edu.eg



Abd Allh Mahrous Abd El-Hamid

Material Science

Nuclear Materials Authority
a.mahrous@nma.org.eg



Hisham Abdallah

Stereochemistry and Enzymes

National Research Center
hishamayosef@yahoo.com



El Sayed Yakout

Organic Chemistry

National Research Centre
sm_yakout@hotmail.com



👤 Hatem A. Abdel Aziz

Organic Chemistry

📍 National Research Center

✉️ hatem_741@yahoo.com



👤 Marwa El Hussieny

Organic Chemistry

📍 National Research Center

✉️ mrw_elhussieny@yahoo.com



👤 Hamdy Zahran

Food Chemistry

📍 National Research Center

✉️ hazahran23@gmail.com



👤 Samir Kamel

Cellulose

📍 National Research Centre

✉️ samirki@yahoo.com



👤 Amgad Al Bohy

Pharmaceutical Chemistry

📍 British University in Egypt

✉️ albohy@ualberta.ca



👤 Sudip Kumar Mandal

Pharmaceutical chemistry (Medicinal chemistry)

📍 Dr. B. C. Roy College of Pharmacy & AHS
Durgapur-713206, W.B., India

✉️ gotosudip79@gmail.com



Omnia Elsaid Shahat

Physical Chemistry

National Research Center
omniashehata@yahoo.com



Nady A. Fathy

Applied Physical Chemistry

Surface Chemistry and Catalysis Laboratory
Physical Chemistry Department,
National Research Center,
EGYPT.
fathyna.77@hotmail.com



Helder T. Gomes

Physical Chemistry

Mountain Research Centre (CIMO)
LSRE-LCM Associate Laboratory
Laboratory of Separation and Reaction Engineering - Laboratory of Catalysis and Materials
Department of Chemical and Biological Technology
Polytechnic Institute of Bragança
Campus Santa Apolónia
5300-253 Bragança, Portugal
CIMO: cimo.ipb.pt LSRE-LCM: lsre-lcm.fe.up.pt
htgomes@ipb.pt
0000-0001-6898-2408



Salwa El-Sabbagh

Polymer Chemistry

National Research Center
salwa_elsabbagh@yahoo.com



Ahmed Goma Hassabo

Textile

National Research Centre
aga.hassabo@hotmail.com



Mohamed Amin El-Shahir

Chemical Engineering

British University In Egypt (BUE)
shahir.sadek@bue.edu.eg



Mona M. Amin

Chemical Engineering

National Research Centre
monaamin46@gmail.com



👤 Mahmoud Saleh

Biochemistry

📍 *Faculty of Science, Cairo University*
✉ msaleh@sci.cu.edu.eg



Coordinator

👤 Shaima Banoon

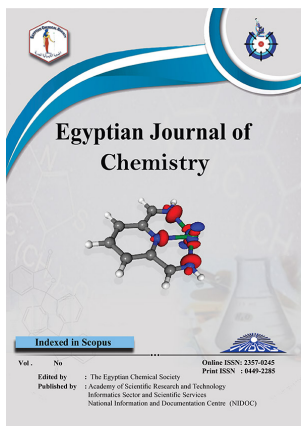
📍 *College of Science, University of Misan, Maysan, Iraq*
✉ shimarb@uomisan.edu.iq
☎ +964 782 827 0929



Assistant Editor

👤 Wesam Said Aboul Anin

📍 *National Information and Documentation Center (NIDOC)*
✉ nidocpub6@gmail.com
☎ 01204797030



Articles in Press

Current Issue

Journal Archive

+ Volume 66 (2023)

- Volume 65 (2022)

- Issue 132
Special Issue: Chemistry and Global Challenges (Part B)
- Issue 131
Special Issue: Chemistry and Global Challenges (Part A)
- Issue 12
- Issue 11
- Issue 10
- Issue 9
- Issue 8
- Issue 7
- Issue 6
- Issue 5
- Issue 4
- Issue 3
- Issue 2
- Issue 1

+ Volume 64 (2021)

+ Volume 63 (2020)

+ Volume 62 (2019)

+ Volume 61 (2018)

+ Volume 60 (2017)

+ Volume 59 (2016)

+ Volume 58 (2015)

+ Volume 57 (2014)

+ Volume 56 (2013)

+ Volume 55 (2012)

+ Volume 54 (2011)

Volume & Issue: Volume 65, Issue 12, December 2022

Number of Articles: 70

Main Subjects

- Analytical chemistry 3
- Biochemistry 13
- Environmental chemistry 8
- Food Chemistry 3
- Inorganic chemistry 1
- Material science 5
- Nano chemistry 3
- Nanotechnology 2
- Organic chemistry 11
- Pharmaceutical Chemistry 5
- Physical chemistry 3
- Polymer chemistry 2
- Textile chemistry 3

Methylene Blue Cationic Dye Removal using AA-Am Hydrogel as An Efficient Adsorbent

Pages 1-10

10.21608/EJCHEM.2022.118700.5344

R. Alaraby; Marwa M. El Sayed

View Article PDF 1.24 MB

Synthesis, DFT, Antibacterial and Molecular Docking Studies of Novel La(III) Complex of Benzo-Chromen Substituted Thiosemicarbazide

Pages 11-19

10.21608/EJCHEM.2022.131586.5798

Eman Fares Mohamed; Safaa Said Hassan

View Article PDF 626.8 K

Visualization the crystal structure, microstructure, magnetic performance and antimicrobial as well as anticancer activities of La_{0.5}Sr_{0.5}Mn_{0.9}Ti_{0.1}O₃ nanopowders

Pages 21-26

10.21608/EJCHEM.2022.130541.5752

Hesham Ahmed Tash; Ali Omar Turkey; Ali Mostafa Hassan; Hosni Anwar Gomaa; Mohamed Mohamed Rashad

View Article PDF 628.75 K Scopus 1

Synthesis of New Organophosphorus Pyrazole Derivatives as Human Myeloblastic Leukemia HL60 Cytotoxic Agents

Pages 27-37

10.21608/EJCHEM.2022.150667.6525

Mansoura Ali; Mohamed El-Gendy

View Article PDF 960.34 K

Synthesis and Antimicrobial Activity of Copper and Zinc Complexes based on Benzimidazole scaffold

Pages 39-47

[doi](https://doi.org/10.21608/EJCHEM.2022.152140.6592) 10.21608/EJCHEM.2022.152140.6592

Nagwa M. Abdelazeem; Farid M Sroor; Mohamed S. Abdel-aziz;
Wahid M. Basyouni

View Article [PDF](#) 661.76 K

Effect of Three Formulations Derived from Plant Origin on Two-spotted Spider Mite *Tetranychus urticae* Koch (Acari: Tetranychidae)

Pages 49-57

[doi](https://doi.org/10.21608/EJCHEM.2022.121372.5442) 10.21608/EJCHEM.2022.121372.5442

Saad El adawey Hamouda; hisham ibrahim Abd-Alla

View Article [PDF](#) 499.59 K

Formulation, Characterization and Insecticidal Effect of Two Volatile Phytochemicals Solid-lipid nanoparticles against some Stored Product Insects

Pages 59-71

[doi](https://doi.org/10.21608/EJCHEM.2022.121873.5509) 10.21608/EJCHEM.2022.121873.5509

Manal M Adel; Shimaa S.I. Abd El-Naby; Khaled H.M. Abdel-Rheim;
nagwa salem

View Article [PDF](#) 370.32 K

Synthesis and Characterization of some Substituted Octahydroquinazoline using Ultrasound Technique

Pages 73-78

[doi](https://doi.org/10.21608/EJCHEM.2022.121240.5439) 10.21608/EJCHEM.2022.121240.5439

Omar Mohammed Yahya; Salim Jasim Mohammed; Attallah
Mohammed Sheat

View Article [PDF](#) 548.32 K

Effect of irrigation water quantity and salinity level on growth and internal chemical contents of Moringa plants

Pages 79-85

[doi](https://doi.org/10.21608/EJCHEM.2022.144021.6283) 10.21608/EJCHEM.2022.144021.6283

Hesham S. Abdelaty; Abdelaziz M. Hosni; Ahmed N. Abdelhamid;
Aboelfetoh Abdalla

View Article [PDF](#) 281.03 K

Effect of Zinc and Boron foliar application on leaf chemical composition of *Moringa oleifera* and on yield and characters of its seed oil

Pages 87-93

[doi](https://doi.org/10.21608/EJCHEM.2022.141002.6164) 10.21608/EJCHEM.2022.141002.6164

Fardous M. Abdelwanis; Abdelaziz M. Hosni; Ahmed N.
Abdelhamid; Ahmad A. Sulman; Mohamed I. Ezoo; Said Abdelhalim
Saleh

View Article [PDF](#) 203.16 K

Synthesis of 3-pentyl-5-(4-chlorobenzylidene)imidazolidine-2,4-dione and 1,3-dipentyl-5-(4-chlorobenzylidene)imidazolidine-2,4-dione

Pages 95-99

[doi](https://doi.org/10.21608/EJCHEM.2022.69081.3512) 10.21608/EJCHEM.2022.69081.3512

muhammad naufal; Irana Rahmawati Sabana; Jamaludin Al-Anshori; Rani Maharani; Achmad Zainuddin; Dadan Sumiarsa; Ace Tatang Hidayat; Ika Wiani

View Article  PDF 848.66 K

Application of Reactive dyes by Dyeing and Printing Method on Cotton Fabric and Study of Antibacterial Activity

Pages 101-110

 10.21608/EJCHEM.2022.101107.4697

Manojkumar J. Patel; R. C Tandel

View Article  PDF 825.05 K

Bis(dibenzoylmethanato)Zirconium(IV) Chloride Complex as a Potential Catalyst for the Ring Opening Polymerization of d-Valerolactone

Pages 111-119

 10.21608/EJCHEM.2022.107965.4942

Muhammad Yusuf; Eddiyanto Eddiyanto; Rudi Munzirwan Siregar; Rizki Dwi Irmalasari

View Article  PDF 803.82 K

Decolorization of Reactive Dyes, Part IV: Eco-Friendly Approach of Reactive Red 195 Dye Effluents Decolorization Using Geopolymer Cement Based on Slag

Pages 121-127

 10.21608/EJCHEM.2022.148302.6411

Morsy Ahmed El-Asasery; Amal A Aly; Doaa Abdel Monem Ahmed

View Article  PDF 665.04 K  4

Decolorization of Reactive Dyes, Part V: Eco-Friendly Approach of Reactive Red 195 Dye Effluents Decolorization Using Geopolymer Cement Based on Metakaolin

Pages 129-135

 10.21608/EJCHEM.2022.149781.6473

Morsy Ahmed El-Asasery; Amal A Aly; Doaa A Ahmed



View Article  PDF 678.25 K  2

Improving the Production of Total Phenolics and Flavonoids and the Antioxidant Capacity of Echinacea purpurea Callus through Biotic Elicitation

Pages 137-149

 10.21608/EJCHEM.2022.145210.6328

Omar A. M. Elshahawy; Mohamed E.-F. Zeawail; Mohamed A. Hamza; Ahmed Abdelfattah Elateeq; Magdy A. Omar

View Article  PDF 743.36 K  1

Engineered Nanomaterials, Plants, Plant Toxicity and Biotransformation: A review

Pages 151-164

 10.21608/EJCHEM.2022.131166.5775

Saade A Jasim; Hamzah H. Kzar; R. Sivaraman; Muhsin J Jweeg; Muhaned Zaidi; Ola Kamal A. Alkadir; Fatima Safaa Fahim; Ahmed Kareem Obaid Aldulaim; Ehsan Kianfar

[View Article](#) [PDF 700.43 K](#) [Scopus](#) 2

Jasonia montana Extracts Stimulate Cell Differentiation in HCT-116 and Caco-2 Cell Lines

Pages 165-174

[DOI](#) 10.21608/EJCHEM.2022.113827.5252

Esraa A. Aidy; Zeinab Fathy; Wafaa Abdullah Ahmed; Saad El-Gendy; Amany Abou-Bakr; Mervat Omran; Tamer A. Al-Shafie

[View Article](#) [PDF 733.65 K](#)

Circulating Irisin In Relation To Obesity and Anorexia Nervosa in Patients with Type 2 Diabetes

Pages 175-180

[DOI](#) 10.21608/EJCHEM.2022.112977.5143

Moushira Zaki; Hanaa Reyad Abdallah; Hala T. El-Bassyouni; HEND M. Tawfeek; Hanan Hanna; Magdi N. Ashour; Eman R. Youness

[View Article](#) [PDF 452.29 K](#)

Dry Powder Inhalation Microparticles (Alginate, Carrageenan, Chitosan, and Combination Polymers): A Review on Characteristics and In Vivo Activity

Pages 181-206

[DOI](#) 10.21608/EJCHEM.2022.119143.5364

Iqlima Prestisya; Andang Miatmoko; Mahardian Rahmadi; DEWI MELANI HARIYADI

[View Article](#) [PDF 680.72 K](#)

Bioactivity and metabolomics fingerprinting characterization of different organic solvents extracts of Padina pavonica collected from Abu Qir Bay, Egypt

Pages 207-225

[DOI](#) 10.21608/EJCHEM.2022.126649.5612

Ahmed Shahin; Asmaa Nabil-Adam; Khaled Elnagar; Hanan Osman; Mohamed Attia Shreadah

[View Article](#) [PDF 796.52 K](#)

Flocculation Activity of Grafted Chitosan for Water Treatment

Pages 227-237

[DOI](#) 10.21608/EJCHEM.2022.119028.5352

Raedah Alatawi; Abeer Abdulaziz Bukhari; Hanan Elsayed; Uzma Faridi; Sanaa Khali; Wael Mohammed

[View Article](#) [PDF 645.35 K](#)

Evaluation of the Sewi dates safety produced by the traditional method

Pages 239-249


[DOI](#) 10.21608/EJCHEM.2022.122952.5501

Gomaa Nour-Eldein Abdel-Rahman; Salah Hamza Elmahdy Salem; Essam Mahmoud Saleh; Daa Attia Marrez

[View Article](#) [PDF 792.86 K](#)

Structure Modification Of MoS₂ Through Preparation Condition Management

Pages 251-257


 10.21608/EJCHEM.2022.124371.5540

H. H. Afify; M. Obaida; Mai N. Swelam; S.A. Hassan; H. M. Hashem; A.,Abd El-Mongy

View Article  PDF 948.57 K

Alkaline Hydrolysis of Polyester Woven Fabrics and its Influence on Thermal Comfort Properties

Pages 259-274


 10.21608/EJCHEM.2022.122214.5508

Alsaid Ahmed Almetwally

View Article  PDF 920.39 K

L-methioninase enzyme production by E. coli WSM2 using some organic by product residues

Pages 275-281

 10.21608/EJCHEM.2022.123441.5517

Afra M Baghdadi; Enas N Danial

View Article  PDF 649.67 K

N-Isopropylacry Amide Nanogel for Surface Treatment of Corroded Copper Ornaments associated on Coptic Linen

Pages 283-294

 10.21608/EJCHEM.2022.128292.5725

neven fahim fahim; Saleh Mohammed Ahmed

View Article  PDF 1.37 MB

Phytochemical and Nutritional Studies of Bottle Gourd (Lagenaria Siceraria Ls) Cultivated In Egyptian Habitat

Pages 295-304


 10.21608/EJCHEM.2022.150722.6528

Abdel-Raheem A. A. Aldewy; Abdelaaty Hamed; Yousry A Ammar; Abdel Mohsen M M Nezam-El-Dien; Mohamed Shaaban

View Article  PDF 693.17 K

Identification and quantitation of ursolic acid in Plectranthus amboinicus extract; molecular docking approach for its antiproliferative potential

Pages 305-311

 10.21608/EJCHEM.2022.124418.5551

Mona AbdelMohsen; Ibrahim Ahmed Salah; Heba Handoussa; Yasmine Mandour

View Article  PDF 717.92 K

Synthesis of Zeolite Beta Using Seawater Instead of Deionized Water

Pages 313-317

 10.21608/EJCHEM.2022.104358.4956

Djamal DARI; Azzeddine Farid Houari; Christian Beling; Fatiha Djafri; Abdelkader Bengueddach; Mohamed Sassi

View Article  PDF 790.14 K

Synthesis and Biological Evaluation of Novel Quinazoline, Chromene and Chromeno[2,3-d]pyrimidine Derivatives

Pages 319-325

 10.21608/EJCHEM.2022.113647.5161

Mahmoud Nabil Mahmoud Yousif; Abdel-Rhman B. A. El-Gazzar; Hend N. Hafez; Nabil M. Yousif



View Article  PDF 462.17 K

Induced Biosynthesis of Acephenanthrylene in Callus Culture of *Pimpinella anisum* L., by Yeast and Phenylalanine Application

Pages 327-335


 10.21608/EJCHEM.2022.124157.5541

Nermeen M. Arafa; Usama I. Aly

View Article  PDF 735.61 K  Scopus 1

Nano micelle: Novel Approach for Targeted Ocular Drug Delivery System

Pages 337-355

 10.21608/EJCHEM.2022.119133.5359

Md Semimul Akhtar; Sudip Kumar Mandal; Akash Malik; Anshika Choudhary; Saiyam Agarwal; Sipra Sarkar; Suddhasattya Dey



View Article  PDF 1.16 MB

Synthesis and Characterization of Chitosan/ZrO₂ Nanocomposite and Its Application in the Removal of Rose Bengal Dye

Pages 357-367

 10.21608/EJCHEM.2022.120576.5408

Ahmed Abdelwakel Thabet; Ahmed Samer Elfaky; Wael Sabry Mohamed; Ahmed El-Zaref; Zein Elbahy

View Article  PDF 970.13 K  Scopus 1

In vitro regeneration and improving kaempferol accumulation in blackberry (*Rubus fruticosus* L.) callus and suspension cultures

Pages 369-383

 10.21608/EJCHEM.2022.118717.5340

Manal El-salato Ala El-naby Ahmed; Tamer Mahfouz Abd Elaziem Abd Elaziem

View Article  PDF 1.08 MB

Natural Dyes Printability of Modified Silk Fabric with Plasma/Nano Particles of Metal Oxides

Pages 385-396

 10.21608/EJCHEM.2022.113249.5145

Hend M. Ahmed; Hanan El-Sayad; Wafaa Raslan; Usama Rashed; Azza El-Halwagy

View Article  PDF 957.19 K

Irisin, an Exercise Stimulated Hormone as a Metabolic Regulator in Metabolic Syndrome in Obese Rats

Pages 397-407

 10.21608/EJCHEM.2022.113904.5247

Wafaa I. Rasheed; Tahany R. Elias; Magdi N. Ashour; Mervat H. Agaiby; Maha Al Wassif; Eman R. Youness; Yassmin Abdel Latif; Noha Nazih

View Article  PDF 1.03 MB

Dual pharmacological targeting of Mycobacterium tuberculosis (Mtb) PKNA/PKNB: A novel approach for the selective treatment of TB illness

Pages 409-419


 10.21608/EJCHEM.2022.135419.5981

Ali N. Hussein; Mohammed FAWZI; Rasha Fadhel Obaid; Shaima Rabeea Banoon; Emad S Abood; Abdolmajid Ghasemian

View Article  PDF 1.07 MB

Effecting the Donor Moieties on the Efficiency of D- π -A System Candidate for Optoelectronic Applications: A DFT Study

Pages 421-428

 10.21608/EJCHEM.2022.102495.4753

Faeq AL–Temime; Faiz Salih Abbas; Ali K. Alsaedi

View Article  PDF 746.63 K

Low Cholesterol Fermented Milk Beverage by Probiotic Bacteria

Pages 429-437

 10.21608/EJCHEM.2022.100475.4668

Nadia Mohamed Shahein; Nabil Samy Abd-Rabou; Mohamed Tawfeek Fouad

View Article  PDF 444.03 K

Promotion of physiological resistance in Phaseolus vulgaris L. seedlings grown under salinity stress conditions by using ascorbic acid and biofertilizers

Pages 439-455

 10.21608/EJCHEM.2022.137319.6059

Abd El-Baki G.K; Doaa Moustafa; Al-Shima Rafat

View Article  PDF 753.11 K

Therapeutic Effect of Equisetum arvense L. on Bone and Scale Biomarkers in Female Rats with Induced Osteoporosis

Pages 457-466

 10.21608/EJCHEM.2022.127817.5699

Eman S. Ibrahim; Ghada H. Mohamed; Aml F. El-Gazar

View Article  PDF 550.91 K

Kinetics of pyrolysis of water hyacinth: A novel empirical approach

Pages 467-479

 10.21608/EJCHEM.2022.125143.5565

jasmine abdelraouf; hanaa mazhr abdelhady; magdi Abadir; Hanem Abdel-ElRahman Sibak

View Article  PDF 871.89 K

Synthesis, Corrosion inhibition study and DFT calculation of two New Azo Compounds

Pages 481-492

 10.21608/EJCHEM.2022.113018.5142

Hawraa K Deaf; Ekhlas Q Jasim; H. Al-Asadi Rafid; K M Mohammed


View Article  PDF 1.06 MB

Modulatory Effects of Cilostazol; an Nrf2/HO-1 activator against NAFLD in Rats Confirmed by Molecular Docking and FTIR Studies

Pages 493-508


 10.21608/EJCHEM.2022.138491.6091

Ahmed A. Sedik; Asmaa A. Amer

View Article  PDF 1.8 MB

Reinforced modified carboxymethyl cellulose films with graphene oxide/silver nanoparticles as antimicrobial agents

Pages 509-518

 10.21608/EJCHEM.2022.157801.6834

Hebat-Allah S. Tohamy



View Article  PDF 1.25 MB

Antioxidant Isoenzymes, Chemical Constituents and Growth Parameters of Cadmium-Stressed *Dimorphotheca ecklonis* Plant and Affected by Humic Acid

Pages 519-532

 10.21608/EJCHEM.2022.119441.5370

Samah Mostafa El-Sayed; Nahed G. Abdel-Aziz; Azza Abd El-Hamid Mazhar

View Article  PDF 612.69 K  1

Efficient Synthesis and Antimicrobial Evaluation of New Organophosphorus Dioxaspirodecanone Derivatives

Pages 533-542


 10.21608/EJCHEM.2022.140804.6159

Hala Ramadan El-Shanawany; Soher Said Maigali; Naglaa Fathy El-Sayed; mohamed adel youssef; Mohamed ELSayed Abdel-Aziz

View Article  PDF 956.42 K

Swift and Enhanced-Sensitive Analytical Method for Determination of Fumonisin FB1 And FB2 in Egyptian Oilseeds Using LC-MS/MS.

Pages 543-554

 10.21608/EJCHEM.2022.129939.5730

atef ahmed badr; Hamdy Ali; Ahmed Abd El-Hakim; Ahmed Mamdouh Goma

View Article  PDF 526.59 K

Functional low-fat labneh fortified with resistant potato starch as prebiotic and assessed physicochemical, microbiological, and sensory properties during storage

Pages 555-568

 10.21608/EJCHEM.2022.157450.6824

Amira salah El-rahmany; Amal Ibrahim El-Dardiry; Amro Abdelazez;
Osama Safwat Fawzy Khalil

View Article  PDF 820.59 K

Synthesis and biological activity evaluation of some novel heterocyclic compounds incorporating pyridine / chromene moiety

Pages 569-576

 10.21608/EJCHEM.2022.127181.5653

Fathy Mohamed Abdel-Razek; Ali M. S. Hebishy; Rewaida H. Ali

View Article  PDF 642.56 K

Design, Synthesis, Molecular Docking of Some New Polyhydrobenzothieno thiazolopyrimidinedione Glycoside Derivatives with Double Anti-microbial-Anti inflammatory Action

Pages 577-598

 10.21608/EJCHEM.2022.155556.6714

Nesrin M. Morsy; Khadiga M. Abu-Zied; Ahmed S. Aly; Abdelbaset M. Elgamal

View Article  PDF 1.18 MB

Influence of Self Adhesion Mechanical and Physical Properties of Palm Trees Fibers - Polystyrene Composites

Pages 599-606

 10.21608/EJCHEM.2022.123682.5524

Laila Reda; Lameas Mohamed; Deia Ibrahim Moubarak



View Article  PDF 769.28 K

Production, Structural properties Nano biochar and Effects Nano biochar in soil: A review

Pages 607-618

 10.21608/EJCHEM.2022.131162.5772

Baydaa Abed Hussein; Ahmed B. Mahdi; Samar Emad Izzat; Ngakan Ketut Acwin Dwijendra; Rosario Mireya Romero Parra; Luis Andres Barboza Arenas; Yasser Fakri Mustafa; Ghulam Yasin; Ali Thaeer Hammid; ehsan kianfar

View Article  PDF 376.79 K  5

Improvement the Drought Tolerance of Eucalyptus citriodora Seedling by Spraying Basil Leaves Extract and Its Influence on Growth, Volatile Oil Components and Some Enzymatic Activity

Pages 619-635


 10.21608/EJCHEM.2022.127566.5662

Shaimaa I.M. Elsayed; Azza A.M. Mazhar; Samah M. El-Sayed; Amr Said Mohamed

View Article  PDF 644.23 K

Characterization of Egyptian Monovarietal Koroneiki Virgin Olive Oil and Its Co-Products

Pages 637-645

 10.21608/EJCHEM.2022.167449.7064

Minar Mahmoud M. Hassanein; Eman Fawzi Al-Amrousi; Ghada A. Abo-Elwafa; Adel Gabr Abdel-Razek

View Article  PDF 338.74 K

Chemical reaction and non-Darcian effects on MHD generalized Newtonian nanofluid motion

Pages 647-655

 10.21608/EJCHEM.2022.132580.5857

Mohamed Abouzeid

View Article  PDF 576.35 K

Submerged Production, Partial Purification and Characterization of Extracellular Chitinase from Local Endophytic Fungus for Culex pipiens Biocontrol: Strategy for Protein Stabilization

Pages 657-669

 10.21608/EJCHEM.2022.129898.5855

Eman W. Elgammal; Eman F. Ahmed; Omnia M.H.M. Kamel; Heba Yehia

View Article  PDF 789.96 K

Influence of magnesium, molybdenum and sulfur sprays on the yield, fruit and oil properties of Coratina olive trees

Pages 671-682

 10.21608/EJCHEM.2022.158076.6841

Hossam El-Attar; hassan sayed hassan; Mohamed maher Saad Saleh; Marwa AbdElhady AbdElfatah; Amal Tag elden

View Article  PDF 537.25 K

Decolorization of Reactive Dyes, Part VI: Eco-Friendly Approach of Reactive Dye Effluents Decolorization Using Geopolymer Cement Based on Metakaolin backed by slag

Pages 683-688

 10.21608/EJCHEM.2022.176459.7223

Sara Morsy Ahmed; Amal A Aly; Morsy Ahmed El-Asasery; Shereen M Ragai

View Article  PDF 384.99 K

Decolorization of Reactive Dyes, Part VII: Eco-Friendly Approach of Reactive Dye Effluents Decolorization Using Geopolymer Cement Based on Metakaolin-Slag mixes

Pages 689-694

 10.21608/EJCHEM.2022.176464.7224

Sara Morsy Ahmed; Amal A Aly; Morsy Ahmed El-Asasery; Shereen M Ragai

View Article  PDF 563.56 K

Phytochemical Profile, Anti-lipid peroxidation and Anti-diabetic activities of Thymus algeriensis Boiss. & Reut

Pages 695-705

 10.21608/EJCHEM.2022.126336.5600

Zaoui Heyem; Boutaoui Nassima; Menad Ahmed; Ramazan Erenler; Zaiter Lahcene; Benayache Fadila; Souad Ameddah

[View Article](#)  PDF 487.95 K

Acrylamide Formation In Cake Baked In Different Utensils And Novel Intervention Strategies

Pages 707-715

 10.21608/EJCHEM.2022.126624.5611

Rasha Alaa El- Deen Shalaby; Dina A. Anwar; Randa Saad Hassan

[View Article](#)  PDF 651.23 K

Ameliorative Impacts of Dactyloctenium aegyptium and Parapholis incurva Ethanolic Extracts on Sodium Fluoride Induced Pathological Alterations in the Thyroid Gland in Male Rats

Pages 717-739

 10.21608/EJCHEM.2022.150491.6522

Shimaa Nabil El-Sayed; Aida Ahmed Hussein; Abdelsamed I. Elshamy; Abde Razik H. Farrag; Rania Abd-ElKarim Ahmed

[View Article](#)  PDF 1.75 MB

Synthesis and Evaluation of the Antiproliferative Potency and Induced Biochemical Parameters of Novel Pyrazolones Derivatives Towards Hepatocellular Carcinoma

Pages 741-749

 10.21608/EJCHEM.2022.126714.5622

abdelmohsen soliman; Hanaa. Roaiah

[View Article](#)  PDF 614.28 K

Profiling of The Essential Oil of Murraya Paniculata Cultivated in Egypt over Four Different Seasons Using Gas Chromatography-Mass Spectrometry and Screening for Antimicrobial and Anticancer Activities

Pages 751-759

 10.21608/EJCHEM.2022.148077.6408

Hala H. Zaatout; Hend A. Al-koriety; Gamal A. Omran; Amira M. Beltagy

[View Article](#)  PDF 627.95 K

Studying the Chemical Composition and Hepatoprotective Activity Of Capparis Sinaica veill towards CCl4 Injury in Albino Rats

Pages 761-767

 10.21608/EJCHEM.2022.143584.6268

Sahar Awad Allah Hussein; Mona Abdalla mousa mohamed; Alaaeldin Sayed Sayed Ewase; Abdelmohsen M. Soliman

[View Article](#)  PDF 739.05 K

Enhancing the biochemical constituents in avocado callus using encapsulated chitosan nanoparticles

Pages 769-782


 10.21608/EJCHEM.2022.113494.5176

Reda Abo El-Fadl; Asmaa Mahdi; Ahmed E. Abdelhamid; Mohamed R Abdel Magid; Ahmed H Hassan

[View Article](#)  PDF 943.06 K

Synthesis of heterocyclic compounds by cyclization of Schiff bases prepared from capric acid hydrazide and study of biological activity

Pages 783-792


 10.21608/EJCHEM.2022.133946.5904

Ahmed Saleh; Mohanad Y. Saleh

View Article  PDF 850.24 K

Synthesis of Nanochitosan membranes from Shrimp shells

Pages 793-798

 10.21608/EJCHEM.2022.134670.5928

Amal Mohammed; Yusra Alobaidi; Hanaa Abdullah

View Article  PDF 663.18 K



Dry Powder Inhalation Microparticles (Alginate, Carrageenan, Chitosan, and Combination Polymers): A Review on Characteristics and In Vivo Activity

Iqlima Ayu Prestisya^a, Andang Miatmoko^a, Mahardian Rahmadi^b, Dewi Melani Hariyadi^{1*}



CrossMark

^aDepartment of Pharmaceutical Sciences, Faculty of Pharmacy, Universitas Airlangga, Campus C Mulyorejo, Surabaya 60115, Indonesia

^bDepartment of Pharmacy Practice, Faculty of Pharmacy, Universitas Airlangga, Campus C Jl. Mulyorejo 60115, Surabaya, Indonesia

Abstract

Dry Powder Inhaler (DPI) delivers one or more drug substances to the site of action through the inhalation route. It is used to treat respiratory diseases characterized by airflow obstruction and shortness of breath, including asthma and chronic obstructive pulmonary disease (COPD), respiratory infections, and cystic fibrosis. The inhalation route offers further potential for systemic drug delivery. DPI products consist of a drug formulation (the drug constituent part) and a container closure system. A DPI drug formulation contains the drug substance and excipients, including a drug carrier. Drug formulation plays an essential role in producing an effective inhalable medication. Formulating dry powders for inhalation involves micronization with various methods using various excipients, such as lipids, lactose, and polymers. Each one offers its unique advantages and disadvantages, depending on the therapeutic agent being formulated. This review will be highlighting the use of biodegradable polymers, such as alginate, chitosan, carrageenan, and combination polymers, in inhalation drug delivery systems. Particularly polymers microparticles, known as microspheres, received much attention because of their sustained and prolonged release properties and their application for targeting respiratory diseases. Moreover, this review will also summarize the in vivo drug deposition, lung localization, and histopathological study of microparticles.

Keywords: microparticles; dry powder inhaler (DPI); carrageenan; alginate; chitosan; in-vivo

1. Introduction

A dry powder inhaler is a device that has been widely used in various respiratory diseases such as asthma and chronic obstructive pulmonary disease (COPD) and respiratory infections, and cystic fibrosis. It delivers active pharmaceutical ingredients (API) substances by inhalation to the target site. It is hoped that the delivered drugs can reach the target and treat the target site appropriately. Dry powder inhalers (DPIs) are currently considered a pulmonary drug administration device with the most significant potential for improved and new therapies.

The use of DPI in this therapy transports various active pharmaceutical ingredients that must-have characteristics such as less than 5-micron size, mucoadhesive material, and different other properties and characterization parameters which will be discussed further in the chapter 2. This

review aims to summarize the DPI mechanism, the use of DPI with various types of biodegradable polymers; such as alginate, chitosan, carrageenan, and combination polymers, in inhalation drug delivery system particularly polymers microparticles as known as microspheres which received much attention because of their sustained and prolonged release properties, and also their application for targeting of respiratory diseases. This review also explains both in vitro tests of DPI microparticles and in vivo test drug deposition, lung localization, histopathological study, and macrophages uptake.

2- Dry Powder Inhaler (DPI) Drug-Loaded Polymeric Microparticles for Inhalation Delivery

Dry powder inhaler (DPI) is one of the inhaler delivery devices commonly and ideally used to generate aerosols that have advantages over nebulizers, such as the convenience of a compact,

*Corresponding author e-mail: dewi-m-h@ff.unair.ac.id

Receive Date: 31 January 2022, Revise Date: 23 July 2022, Accept Date: 29 March 2022

DOI: 10.21608/EJCHEM.2022.119143.5364

©2022 National Information and Documentation Center (NIDOC)

portable device and rapid medication delivery in the pulmonary route [1]. It is a breath-actuated device developed to overcome the difficulty of achieving the proper hand–breath coordination required to actuate a pMDI device for effective drug delivery in the lungs. Moreover, some DPI devices emit inspiratory-flow signals that promote suitable techniques and patient adherence. A DPI device consists of a medication reservoir, air inlet, deagglomeration compartment, and mouthpiece. Drug formulations for DPIs are micronized drug particles either in a pure form or bound to an inert, larger carrier molecule to form loose agglomerates. Rapid patient inspiration passes the drug formulation through a screen of spinning surfaces or generates turbulent airflow that disaggregates drug particles into a respirable dose [2].

Medication delivery depends on the peak inspiratory flow rate (PIFR) that a patient can generate through the device. This threshold peak inspiratory flow is, in turn, dependent on the internal resistance of the inhaler and is thus device-specific. A patient-generated PIFR of greater than 60 L/min is considered ideal for the use of most DPI devices. Conversely, a PIFR of less than 30 L/min may be insufficient for optimal pulmonary deposition, while 30–60 L/min rates may still provide sufficient therapeutic effects [2].

Sham et al. (2004) developed a platform for aerosol delivery of nanoparticles by preparing carbohydrate (e.g., lactose) carrier particles containing nanoparticles using a spray-drying technique. Carrier particles can be fabricated with an appropriate MMAD to optimize lung deposition. Dispersion of the lactose carrier containing either gelatin or poly butyl cyanoacrylate nanoparticles by a DPI showed a fine particle fraction (FPF) of about 40% [3]. Upon reaching the deep lung and igniting with the aqueous lining fluid of the lung epithelium, the carrier particles dissolved and released the drug of nanoparticles. A novel type of effervescent carrier particle-containing nanoparticles with an MMAD suitable for deep lung delivery was reported by Ely et al. (2007). Effervescent technology incorporation into the carrier particles added an active release mechanism for nanoparticles after pulmonary administration using DPI [4].

Available DPIs are single and multiple-dose devices. DPI has to be loaded before each inhalation in single-dose products, with a capsule containing powder. After loaded, the capsule is perforated within the device, and the powder is inhaled. Loading, piercing and discarding the capsule require manual dexterity and strength, which can be a problem for the elderly and patients with severe shortness of breath. Even there have been reports of patients swallowing the capsules instead of inhaling the contents. In addition, patients may need to take two or more breaths to inhale the therapeutic dose from the device caused

by high internal resistance. As a precaution, patients should be instructed to check the capsule in the device after the first inhalation and repeat the inhalation process if the capsule is not empty. Labeling one single-dose device to deliver formoterol fumarate stipulates refrigeration of the medication capsules before dispensing. The need for such additional steps and instructional measures may contribute to an already cumbersome process and lead to poor acceptance by patients. Multiple-dose DPI devices either deliver an individual dose of powder from a reservoir (e.g., Turbuhaler) or deliver premeasured individual doses from blisters, disks, or strips (e.g., Diskhaler). Patients tend to favor multiple-dose devices due to their ease and quick use, generally lower costs, and integral dose counters that allow them to view the remaining medication level.

2.1 Inhalation Delivery

It is well known that drugs administered by this route of pulmonary delivery are readily absorbed through the alveolar region directly into the blood circulation. Pulmonary drug delivery systems offer many advantages, such as an absorption area of up to 100 m² with a thin absorption membrane (0.1–0.2 μm) and a low blood supply. The required dose is lower than the oral dose so that side effects can be minimized, the onset of action is speedy, degradation of the drug by the liver is also unavoidable. In addition to these advantages, the delivery of drugs in the lungs also has many influencing factors.

2.1.1 Factors Influence Inhalation Delivery

The physiological factors affect the therapeutic effectiveness of inhalation drug delivery, including aerosol particle size, airway geometry, lung clearance mechanisms, and lung disease [5].

Aerosol particle size

One of the essential variables in determining the deposited dose and the distribution of drug aerosol in the lungs is aerosol particle size. Fine aerosols are distributed on the peripheral airways however store less drug per unit surface area than larger particle aerosols but on the larger particle more central airways. Most therapeutic aerosols are almost always heterodisperse, consist of varying particle sizes and are described by a log-normal distribution with the log of the particle diameters plotted against the number of particles, surface area, or volume (mass) on a linear or probability scale and expressed as absolute values or cumulative percentages. The particle size is determined from this distribution by several parameters. First is the mass median diameter of an aerosol. The aerodynamic diameter relates to a particle of a spherical diameter with a unit density that has the same depositional velocity as the desired particle regardless of its shape or density.

Second, the geometric standard deviation (GSD) measures the particle diameter variability in the aerosol and is calculated from the particle diameter ratio at the 84.1% point on the cumulative distribution curve to the MMAD. The GSD is the same for a log-normal distribution sum, surface area, or mass distribution. GSD's value is 1 indicates monodispersed aerosol, while GSD's more than 1.2 indicates heterodispersion aerosol. Most particles, more than 10 μm , are deposited in the oropharyngeal region with large amounts impacting the larynx, especially when the drug is inhaled from devices requiring a high inspiratory flow rate (DPIs). The large particles are subsequently swallowed and contribute minimally, if at all, to the therapeutic response. Particles 1–5 μm in diameter are deposited in the small airways and alveoli with >50% of the 3 μm diameter particles deposited in the alveolar region. In the case of pulmonary drug delivery for systemic absorption, aerosols with a small particle size would be required to ensure peripheral penetration of the drug. Particles lower than 3 μm have an approximately 80% chance of reaching the lower airways, with 50–60% deposit in the alveoli. However, the most effective particle size for treating systemic diseases has not been determined.

Airway geometry

Branching and narrowing of the airways encourage the impaction of particles. The larger the particle size, the greater the velocity of the incoming air, and the smaller the airway radius, the greater the probability of deposition by impaction. The lung has a relative humidity of approximately 99.5%. The addition and removal of water can significantly affect the particle size of a hygroscopic aerosol and thus deposition [5]. Drug particles are known to be hygroscopic and grow or shrink in size in high humidity, such as in the lung. A hygroscopic aerosol delivered at relatively low temperature and humidity into one of high humidity and temperature would be expected to increase in size when inhaled into the lung. The increase in particle size above the initial size should affect the amount of drug deposited, particularly the distribution of the aerosolized drug within the lung. Ferron et al. have predicted that for initial sizes between 0.7 μm and 10 μm , total deposition of hygroscopic aerosols increases by a factor of 2. However, for NaCl particles with an initial size of 0.1 μm , the distribution pattern in the airways was similar to that for non-hygroscopic particles of the same size with diffusion remaining the primary mechanism of deposition. The total deposited dose may decrease, but the resolution of current imaging techniques is not significant enough to distinguish the shifts in generations in this peripheral lung region. For particles with an initial size of 1 μm , we predict changes in the distribution pattern due to particle growth. The calculations showed a shift from

sedimentation to primary impaction on more central airways [5].

Lung clearance mechanisms

Once the inhaled drug is deposited in the lungs, either cleared from the lungs, absorbed into the systemic circulation, or degraded via drug metabolism, particles of drugs deposited in the conducting airways are mainly removed through mucociliary clearance and, to a lesser extent, are absorbed through the airway epithelium into the blood or lymphatic system. Ciliated epithelium extends from the trachea to the terminal bronchioles. Insoluble particles are trapped in the gel layer of mucus. They are moved toward the pharynx (and finally to the gastrointestinal tract) by the upward movement of mucus produced by the beating of metachronous cilia. In the normal lungs, the rate of mucus movement varies according to the airway area and is determined by the number of ciliated cells and their beat frequency. Movement is faster in the trachea than in the small airways and is affected by ciliary functioning and mucus quantity and quality [6]. For average mucociliary clearance to occur, airway epithelial cells must be intact, ciliary structure and activity normal, the depth and chemical composition of the sol layer optimal, and the rheology of the mucus within the physiological range. Mucociliary clearance is impaired in lung diseases such as immotile cilia syndrome, bronchiectasis, CF, and asthma. In CF, the ciliary structure and function are normal, but the copious amounts of thick, tenacious mucus present in the airways impair their ability to clear the mucus effectively.

Lung disease

Lung diseases (i.e., cystic fibrosis/CF, chronic obstructive pulmonary disease/COPD, asthma, and bronchiectasis) alter the architecture of the lung through changes in bifurcation angles and airway obstruction due to mucus accumulation modifying aerosol deposition and distribution patterns. A decrease in the cross-sectional area of the lung caused by obstruction increases air velocity and turbulence in areas where the airflow is usually laminar. Airway obstruction diverts inspired air to unobstructed airways. Thus, the minimal drug is deposited in the blocked sites, and often it needs to be reached to achieve an optimal therapeutic effect of the drug. In an obstructed lung, the aerosolized drug will be deposited more centrally in the lungs by inertial impaction compared with the uniform distribution achieved in the normal lung [7].

2.2 DPI Polymeric Microparticles

2.2.1 Alginate Microparticles

The use of alginate polymers in microparticles for inhalation drug delivery has begun to be widely studied. Alginate is a polymer polysaccharide, alginate as a matrix due to its biodegradable nature, derived from nature; therefore, it has nontoxic

properties or no subacute/chronic toxicity or carcinogenicity reactions, no risk of immunosuppression, is expected to achieve the ideal local release effect: better biocompatibility

and good stability to avoid second operative resection; as well as low cost and good economic benefits. The following table summarizes various studies that examine the use of alginate.

Table 1: The use of Alginate Microparticles for inhalation

No	Drug	Method	Results	References
1	Paclitaxel	Emulsification/gelation	<ul style="list-style-type: none"> - It is a continuous and direct pathway for lungs chemotherapy. - In endotracheal delivery, PTX-ALG-MPs diminish the drug loss during application. - Encapsulation of alginate microparticles resulted in a better lung tissue AUC with a longer residence time. 	[8]
2	Bovine Serum Albumin (BSA)	Spray-Drying	<ul style="list-style-type: none"> - Particles size suitable for deep lung administration. - The addition of zinc causes a more collapsed geometry. - Protein release depended on the (i) alginate: ZnSO₄ ratio, (ii) BSA content, (iii) type of release medium (rising release rate with rising phosphate concentration). 	[9]
3	Hyaluronic acid	The internal setting, ionotropic gelation with subsequent drying using supercritical CO ₂	<ul style="list-style-type: none"> - The Association of HA with Alginate showed a positive effect in lessening the particles' agglomeration and improving biodegradation. - Physicochemical and aerodynamic properties suitable as a drug carrier for the pulmonary tract. 	[10]
4	Salbutamol sulfate (SBS)	Melting, blending, freezing, powdering, and sieving	<ul style="list-style-type: none"> - Hydrophilic matrix prolongs hydrophilic drug diffusion path. - In vitro dissolution study indicates that when the ratio of the hydrophilic polymer is equated, the drug release will take a long time. - The amount of alginate aid in H-bonding increases the miscibility of alginate and PEG6000 for the former and electrostatic interactions between SBS and alginate for the latter. 	[11]
5	Ciprofloxacin HCl	Ionotropic gelation	<ul style="list-style-type: none"> - The polymer concentration affected the drug release pattern of microspheres but did not affect the particle size. - All formulas produced small size particles which fulfilled the lung region. - Drug release from ciprofloxacin HCl-alginate microspheres followed the Matrix-Higuchi model (diffusion-controlled drug release mechanism). - The highest concentration of alginate polymer in the formula (more than 0.75%) 	[12]

			<p>had the best flow property and demonstrated suitable free flow property.</p> <ul style="list-style-type: none"> - The selected best ciprofloxacin HCl-alginate microspheres issued significant inhibition of microbial against <i>S. aureus</i> ATCC 25923 and <i>P. aeruginosa</i> ATCC 27853. 	
6	Ropinirole hydrochloride (RH)	Spray-drying	<ul style="list-style-type: none"> - The inlet temperature had a remarkable effect on the morphology and yield of the spray-dried microparticles. - On the microparticles' morphology, size, and size distribution, and alginate to drug ratio of 90:10 (w/w) was considered the best formulation. - X-ray diffraction studies showed the spray-dried microparticles were stable for at least two months. - The release rate of RH was significantly affected by polymer concentration in the formulation. 	[13]
7	Ciprofloxacin HCl	Dropping, emulsification	<ul style="list-style-type: none"> - Solvent engineering during the ionic gelation process enables a high degree of molecular encapsulation from low to high molecular weight. - Co-immobilization of an antibiotic, CIP, an enzyme, and AL (Alginate Lyase), was achieved without losing their activities. - The blend microspheres appeared a controlled release profile of active CIP and AL molecules in a simulated gastrointestinal environment. - The incorporation of HMP into the matrix allowed the release of both charge molecules and provided a protective mechanism to negligibly prevent AL inactivation under acid conditions (stomach). - The inclusion of AL in the microsphere biomatrix formulation does not influence CIP antimicrobial activity. However, it improves its release profile at simulated intestinal conditions. 	[14]
8	Salbutamol Sulphate	Prilling, inkjet printing	<ul style="list-style-type: none"> - Particles produced by thermal inkjet printing and aerogel technology are unique nanostructures (highly porous and spherical alginate-based microspheres). - Process development unveiled a feasible printability region limited by ALG concentration in the printable aqueous fluid. - The optimized biopolymer aerogel particle 	[15]

			<p>formulation has excellent and homogenous textural properties falling in the nanoporous range with narrow particle size distribution ($23.8 \pm 4.5 \mu\text{m}$).</p> <ul style="list-style-type: none"> - The processing technique is compatible with incorporating a bioactive compound (salbutamol sulfate) in the aerogel carrier for concealed sustained release. 	
9	Roflumilast	Emulsified spray-drying	<ul style="list-style-type: none"> - The particle size and SPAN values for the crosslinked spray-dried alginate particles were more extensive than microparticles composed without a crosslinking agent. - The formulation prepared using β-cyclodextrin as a carrier (CD formulation) had an enormous particle size value and a more controlled drug release pattern than those made using lactose, mannitol, and maltodextrin as carriers. - The CD formulation with spherical-shaped microparticles gradually bloats to reach its maximum size within three hours. - Analysis of the aerodynamic data for the selected formulation revealed its efficient aerosolization compared to a pure drug for deposition in the alveolar region. - The selected CD formulation had a strong inhibitory effect on the growth of A549 cells compared to the pure drug. Furthermore, they had a marked inhibitory effect on pro-inflammatory cytokines (TNF-α, IL-6, and IL-10) in A549 cells. 	[16]

2.2.2 Chitosan Microparticles

Table 2: The use of Chitosan Microparticles for inhalation

No	Drug	Method	Results	References
1	Fluticasone and (FLU) Salmeterol xinafoate (SX)	Ionotropic gelation	<ul style="list-style-type: none"> - SEM images proved the spherical shape, the FLU and SX loading process in these formulations showed an increase in drug encapsulation within the MPs' networks with increasing drugs concentration. - FLU microencapsulated in an amorphous form in the acrylic derivatives, whereas in CS, CS-tAcon, and CS-Succ, the encapsulation was induced mainly in crystalline form. - In vitro release studies revealed a substantial increase in the dissolution of both drugs from all CS derivatives. The release rate is much higher for SX drugs due 	[17]

			<p>to their complete amorphization, following a similar release rate pattern across all derivatives.</p> <ul style="list-style-type: none"> - CS-g-PHEA and CS-g-PAA derivatives are more promising due to their advanced FLU release profile. 	
2	Isoniazid and Rifabutin	Spray-drying	<ul style="list-style-type: none"> - Inhalable CS has a drug association efficiency of 93% (INH) and 99% (RFB). - The microparticles developed display MMAD around 4 μm and FPF of approximately 45%, suitable for deep lung delivery. - Cytotoxicity assays demonstrated that the formulation is well tolerated by alveolar epithelial cells. - A marginal decrease in cell viability of macrophage-like cells (to 60%) was observed at the highest microparticle concentration tested (1.0 mg/mL) after 24 h exposure. However, this dose is feasibly overestimated compared to actual conditions in vivo. 	[18]
3	Prothionamide (PTH)	Ionic gelation	<ul style="list-style-type: none"> - The prepared PTH nanoparticles were spherical with a particle size of 314.37 ± 3.68 nm. - Optimized PTH nanoparticles have an aerodynamic particle size of 1.76μm and signify their suitability for effective delivery for pulmonary administration. - In-vitro release study indicated the release occurred due to a combination of erosion and diffusion mechanism followed by the Korsmeyer-Peppas kinetic model. - Particle sizes were changed in a narrow range during storage time, but it did not significantly affect the release of PTH from Chitosan nanoparticles. - Prepared DPI prolonged PTH concentration above the MIC for more than 12h after single-dose administration and can raise the treatment's effectiveness by increasing PTH concentration in the lungs tissue with a reduced dose. 	[19]
4	Bovine serum albumin (BSA)	Physically crosslinked hydrogel, graft copolymerization	<ul style="list-style-type: none"> - The hydrogel microparticles were designed in such a fashion to offer good aerodynamic properties (10.01 ± 0.45 and 13.73 ± 0.07 μm) that can confer sustained release of drug once deposited in the lung. 	[20]
5	Clindamycin HCl	Spray-drying	<ul style="list-style-type: none"> - The formaldehyde (crosslinking agent) concentration affected prepared 	[21]

			<p>microspheres' particle size and drug release behavior.</p> <ul style="list-style-type: none"> - Spray drying technology has remained as individual entities with less aggregation. - The characterization of microspheres in terms of size and shape showed that the spray drying technique is handy for manufacturing inhaled powders. 	
6	Levofloxacin	Spray-drying	<ul style="list-style-type: none"> - Spray-dried microparticles containing octanoyl chitosan proclaimed a greater dispersibility and higher FPF when compared to non-modified chitosan. - Morphological investigation showed that the engineered particles have a suitable aerodynamic particle size and relatively low physical contact due to the layers on their surface, leading to a decreased density and hence high dispersibility. - Spray-dried formulations containing octanoyl chitosan were comparable with those containing L-leucine, showing effectiveness as a dispersibility enhancer. - Chitosan hydrophobically modified has dispersibility enhancement property compared to the model hydrophobic amino acid L-leucine due to its antibacterial and mucoadhesive properties. - Mucoadhesion will increase the residence time of the formulations in the lungs, thereby increasing the efficiency of antibiotics to treat infections. 	[22]
7	Rifampicin (RIF) and Rifabutin (RFB)	Ionotropic gelation, spray-drying	<ul style="list-style-type: none"> - Have excellent aerodynamic characteristics, as evidenced by their deposition in the later stages of the ACL. - Chitosan-based microparticles containing antitubercular drugs are nontoxic to the lung tissues. However, repeated-dose inhalation toxicology studies of these formulations will be needed to assess their durable safety better. - The microparticles are also taken up by alveolar macrophages, thus enabling targeting of the <i>Mycobacterium tuberculosis</i> occupying within the macrophages. - Antitubercular drug microparticles, RIF and RFB, are excellent for direct delivery to the lungs when formulated as dry powder for inhalation (DPI). 	[23]
8	Rifampicin	Ionic gelation probe sonication method	<ul style="list-style-type: none"> - The size range and entrapment efficiency of prepared nanoparticles were estimated from 	[24]

			<p>124.1±0.2 to 402.3±2.8 nm and 72.00±0.1%.</p> <ul style="list-style-type: none"> - The nanoparticle formulation was used to conduct in vitro lung deposition studies via Andersen cascade impactor (ACI). - The cumulative in vitro drug release studies with developed nanoparticle formulation demonstrated sustained release for up to 24 hours. - Pharmacokinetic and toxicity studies carried out with prepared NPs DPI formulations compared with conventional DPI marketed formulation showed RFM release for an extended period. 	
9	Insulin	Supercritical fluid assisted atomization	<ul style="list-style-type: none"> - Well-defined spherical TMC microparticles with maintained structure and thermal stability could be obtained. - SAA-HCM proved to be a promising method without using any organic solvents. - The MMAD of the amorphous composite microparticles is within 1-5 µm, which is advantageous for inhalation therapy with rapid dissolution. - In rats, intratracheal administration of TMC/insulin formulations enhanced insulin absorption with relatively higher bioavailability. 	[25]

2.2.3 Carrageenan Microparticles

Table 3: The use of Carrageenan Microparticles for inhalation

No	Drug	Method	Results	References
1	Isoniazid	Emulsification	<ul style="list-style-type: none"> - Various concentrations of surfactant and polymer controlled the sizes of the microspheres. - The absorption of isoniazid into the microspheres depends on the concentration of isoniazid solution. The higher the concentration of isoniazid solution, the higher the percent encapsulation. - The stability of the microsphere depends on crosslinking and the concentration of isoniazid in the solution. The higher the concentration of isoniazid solution, the lower the stability. 	[26]
2	Ciprofloxacin HCl	Ionotropic gelation	<ul style="list-style-type: none"> - Ciprofloxacin HCl-Carrageenan microspheres resulted round spherical shape with a smooth surface. - Increasing the concentration of carrageenan polymers (0.5 to 1.0%) and KCl crosslinker (0.2 to 0.6%) increased particle size, yield, 	[27]

entrapment efficiency, and drug loading.

3	Isoniazid and Rifabutin	Spray-drying	<ul style="list-style-type: none"> - CRG/INH/RFB microparticles were efficiently associated with the model drugs, which antibacterial effect was not affected antibacterial effect. - A common toxic effect was observed in alveolar epithelial cells and macrophages, but further testing is needed. - CRG microparticles demonstrated some ability to interact with macrophages and induced moderate activation of these cells. 	[28]
---	-------------------------	--------------	--	------

2.2.4 Combination Polymer Microparticles

Table 4: The use of Combination Polymers Microparticles

No	Drug	Polymer	Method	Results	References
1	Tobramycin	Alginate-Chitosan	Cationic crosslinking	<ul style="list-style-type: none"> - The formulations showing mucoadhesive properties and the conjugation of SLPI strengthen it. - The particles reported herein could deliver a potent antimicrobial (tobramycin) to <i>P. aeruginosa</i> and dormant increase drug delivery efficacy over prolonged periods. 	[29]
2	Ethionamide	Carrageenan stabilized, Alginate-Chitosan	Ionotropic gelation	<ul style="list-style-type: none"> - Carbohydrate-based polymers are due to their biodegradability and safety, and good physical characteristics. - The physical properties of the nanoparticles, including particles size, shape, and zeta potential, are promising for further researches. - Abilities to reach a reasonable entrapment, a controlled drug release, and a comparable antimycobacterial activity such as <i>Tuberculosis</i>. 	[30]
3	Tobramycin	Alginate-chitosan	Isothermal titration calorimetry	<ul style="list-style-type: none"> - The flexibility of tobramycin NPs by designing a dual-modality NPS incorporating DNase exhibits the effective penetration and anti-pseudomonal activity in the sputum of CF patients. - Tobramycin polymeric NPs have high antibiotic loading, stability, and mucus penetration abilities. 	[31]
4	Losartan	Chitosan-Dextran Sulfate	Spray-drying	<ul style="list-style-type: none"> - LS-MC-DPI exhibited complete burst release during the first 2 h (>95% within 30 min), and LS-MC- 	[31]

				<p>DPI was revealed as a continuous release, accounting for 61.47% throughout 24 h.</p> <ul style="list-style-type: none"> - It showed favorable PS and morphologic structure, reasonable flowability, swelling, mucoadhesive potentials, and sustained drug release. - Superior in vitro lung deposition and tolerability were attained.
5	Budesonide	Alginate-chitosan	Cation induced gelification	<p>- The DPI formulation results were primarily influenced by calcium chloride and chitosan. [32]</p> <ul style="list-style-type: none"> - Main correlations between the flowability, surface charges, and physical properties compared to particle size for particle dynamics in the respiratory tract. - With effective fluidization, particle trajectories, and morphological properties, there was a higher probing effect of surface charge than the formulated DPI and acts as a standard evaluation of lung deposition.
6	Vancomycin	Alginate-chitosan	Emulsion crosslinking	<p>- Vancomycin-loaded alginate-chitosan microspheres having mean particle size and drug loading were $25.3 \pm 5.4 \mu\text{m}$ and $18.5 \pm 2.3\%$. [33]</p> <ul style="list-style-type: none"> - The kinetic profile of vancomycin microspheres indicated a sustained release of the drug. - The higher AUC and the encapsulated half-life of vancomycin propose a longer duration of action than free vancomycin.
7	Resveratrol and Curcumin	Alginate-CMC	Spray-drying	<p>- Improved encapsulation efficiency with 82.91% for resveratrol (in the core) and 59.64% for curcumin (in the shell of the microcapsules) were obtained. [35]</p> <ul style="list-style-type: none"> - In vitro release profiles under simulated gastric and intestinal conditions confirmed controlled release of resveratrol encapsulated in core (or interior surface) of the microcapsules resulting from the 3FN process compared to resveratrol from the microparticle matrix generated from the 2FN spray drying

				<p>process.</p> <ul style="list-style-type: none"> - Curcumin from both formulations showed a slower cumulative release compared to resveratrol. - Both bioactive fit a Korsmeyer-Peppas release kinetic model with a pseudo-Fickian diffusion mechanism for resveratrol and anomalous diffusion for curcumin. - Co-encapsulation did not affect the release profiles of individual bioactive molecules. 	
8	Doxorubicin	BSA, Alginate and Chitosan	Co-precipitation	<ul style="list-style-type: none"> - Owing to the charge variability of BSA with changing pH, the pH-controlled loading effect and release behavior were observed. - Real-time biodistribution of DOX showed the metabolism of DOX-loaded BSA-gel-capsules(MPs) over 48 h post-injection. 	[36]
9	Acetylsalicylic acid (aspirin)	Alginate-pectin	Internal gelation	<ul style="list-style-type: none"> - Drug release is influenced by the medium condition and the properties of the polymer and drug. - More drug release was obtained for an acidic pH environment, and also, the increase in pectin soared the percentage of drug release. The drug release process was affected by the physical and mechanical properties of the gel barrier created around the capsules. - Enhancement of pectin led to poor gel barrier and increased the drug release percentage. - The addition of pectin amounts in the microcapsule increased the particle size and size distribution broader. - Having porous microstructure morphology of alginate pectin microcapsules and also the presence of drug crystals. - Controlled drug release was achieved for up to 350 min by the moderate increase from time to time for the alginate pectin combinations and three pH levels. 	[37]

2. In Vivo Drug Deposition, Lung Localization, Histopathological Study

Table 5: Drug Deposition of Microparticles

No	Drug	Polymer	Method	Main Parameter	References
----	------	---------	--------	----------------	------------

1	Paclitaxel	The sodium salt of alginic acid (Na-Alg) and hydroxypropyl methylcellulose (HPMC)	Aerodynamic assessment of fine particles using a Model DP-4 dry powder insufflator for a rat.	<ul style="list-style-type: none"> - SEM of alginate microparticles has a diameter of less than 5 μm. Maximum drug loading and encapsulation efficiency was 61%. In vitro cytotoxicity of paclitaxel against tumor cell lines agrees with the mechanism of action of paclitaxel. In more extended incubation periods, a more significant number of cells enter the G2 and M cell cycle phases, during which paclitaxel is more active. Fine particle fractions (FPF) (<5 m) were found to be $13.9 \pm 0.57\%$. - Mass median aerodynamic diameters (MMAD) and geometric standard deviation (GSD) were 5.9 ± 0.33 and $1.84 \pm 0.14 \mu\text{m}$. - The percent emitted fraction was 92% 	[8], [38]
2	Bovine serum albumin (BSA)	Sodium alginate	In vitro using a Multi (5)-stage Liquid Impinger.	<ul style="list-style-type: none"> - A decrease in the alginate: ZnSO_4 ratio led to an increase in particle size from 2.9 (± 2.1) μm (10:1 ratio) to 5.0 (± 2.2) μm (1:1 ratio) with spherical shape. - In vitro aerosolization and aerodynamic flow behavior: The addition of $\text{Zn}(\text{NH}_3)_4\text{SO}_4$ to the spray-drying solution during microparticle preparation resulted in a remarkable increase in the FPF (to 32.8% at alginate: ZnSO_4 ratio of 10:1, and to 40.4% at alginate: ZnSO_4 ratio of 2:1). 	[9]
3	Rifampicin-loaded liposomes	Chitosan and k-carrageenan	Powder aerosol performances using a next-generation impactor and a Turbospin as the inhaler device.	<ul style="list-style-type: none"> - The acceptable particle dose and the fine particle fraction were $\sim 1.5 \text{ mg}$ and 50%, respectively, denoting positive aerosol performances for both coated formulations. - Both coated formulations' mass median aerodynamic diameter was much lower ($\sim 2 \mu\text{m}$) than uncoated liposomes ($\sim 9 \mu\text{m}$). - Drug dispersion showed substantial toxicity ($\sim 40\%$) after 2 h incubation and increased to $\sim 65\%$ after 48 h. - Rifampicin-loaded uncoated- and coated-liposomes did not cause significant cytotoxic activity during the first 4 h incubation (less than 15% mortality), and it slowly 	[39]

				increased up to ~30% after 48 h.
4	Bovine serum albumin (BSA) and fetal bovine serum (FBS)	Chitosan, pentasodium tripolyphosphate and κ-carrageenan	Aerodynamic characterization using a TSI Aerosizer LD equipped with an Aerodisperser and assuming actual density as the density parameter to determine the aerodynamic diameter.	<p>- The protein-loaded nanoparticles resulted in a dry powder with suitable properties for lung delivery.</p> <p>- The pulmonary administration of nanoparticles is severely hindered by their low inertia, which makes alveolar deposition practically impossible, mainly resulting in the exhalation of the carriers.</p> <p>- The spray-drying of CS-based nanoparticles can reach the deep lung.</p> <p>- The nanoparticle carriers were determined to have a Feret diameter of $2.3 \pm 0.6 \mu\text{m}$, an absolute density of $1.44 \pm 0.01 \text{ g/cm}^3$ and a tap density of $0.42 \pm 0.04 \text{ g/cm}^3$. The aerodynamic diameter was determined to be $1.80 \pm 0.11 \mu\text{m}$.</p>
5	Fraction V Bovine Serum Albumin (BSA)	Chitosan, Alginate, PLGA, Gelatin, HPC-L, Ovalbumin, Sodium hyaluronate	Aerosolization efficiency aerosolized at 60 l/min through a DPI using an Andersen cascade impactor.	<p>- The fine particle fraction (FPF) was highest in the case of HPC-L particles (26.1%) and lowest with ovalbumin particles (11.9%). The other polymers produced FPF values between 14 and 21%.</p> <p>- The MMAD values were more prominent than the theoretical; between 2.9 and 4.7 m, possibly due to particle aggregation.</p> <p>- Emitted dose uniformity for all formulations as tested using DUSA were in the acceptable range (80.9–91%). The values were $82.4 \pm 7.5\%$ (chitosan), $84.4 \pm 6.1\%$ (alginate), $85.5 \pm 8.7\%$ (PLGA), $80.9 \pm 2.3\%$ (gelatin), $91.1 \pm 4.5\%$ (HPC), $81.3 \pm 3.2\%$ (ovalbumin), and $80.2 \pm 2.6\%$ (sodium hyaluronate).</p>
6	Hyaluronic acid (HA)	Sodium Alginate (Alg)	Aerodynamic properties were estimated by the d_A , while dv of the aerogel microspheres was calculated from the particle size distribution data measured with a Camsizer XT.	<p>- The mean particle diameter of the Alg microspheres decreased from 51.4 ± 12.6–$22.5 \pm 0.7 \mu\text{m}$, and the Alg-HA microspheres from 40.0 ± 0.8–$33.0 \pm 8.8 \mu\text{m}$, caused by the stirrer rate were increased from 850 to 1200 rpm. The experimental d_A values for the Alg microspheres were well estimated, except for sample 1% Alg₁₂₀₀, which has the smallest dv of $22.5 \pm 0.7 \mu\text{m}$ that</p>

				might lead to aggregation of the solid microspheres because of the high surface energy, which increases the experimental d_A values.	
7	Budesonide	Sodium alginate-chitosan	In vitro deposition study uses an eight-stage, non-viable cascade impactor. In water, the impaction plates were precoated with a 1.5% (w/v) of HPMC (4000 Hz) gel. In vivo lung deposition fraction: Healthy male Wistar albino rats weighing between 250 and 350 g were used for lung deposition fraction study. They were maintained in cages with a preserved 12: 12 h dark/light cycle and free access to standard food and tap water.	- The MMAD of obtained budesonide and commercial DPI were of 1.16 ± 0.01 and $5.04 \pm 0.03 \mu\text{m}$, which was an acceptable range (0.5 to $5 \mu\text{m}$) for the lung deposition. - The fine particle fraction reached the lower seven stages of the impactor (corresponding to aerodynamic diameters $<5.8 \mu\text{m}$) or the lower five stages (corresponding to aerodynamic diameters $<3.3 \mu\text{m}$). The lower MMAD was also reflected in fine particle fraction, $56.18 \pm 0.01\%$ for obtained DPI and $22.83 \pm 0.02\%$ for commercial DPI, respectively. - The improved deposition fraction in the tracheobronchial area of formulated budesonide loaded biopolymer DPI attributes better aerodynamic behavior such as less MMAD ($1.16 \pm 0.01 \mu\text{m}$), deaggregation, and better flowability.	[33]
8	Roflumilast	Alginic acid sodium	The MKII ACI consists of an induction port, pre-separator, stage-0 to stage 6 and filter. The selected formulation (10 mg) and the pure drug were filled separately into size-3 hard gelatin capsules. DPI was loaded at a flow rate of 60 L/min with a flow duration of 4 sec.	- The microparticles had the highest deposition in stage 3 (particles between $3.4\text{-}4.6 \mu\text{m}$) and stage 4 (particles between $2.1\text{-}3.2 \mu\text{m}$) of the ACI, most relevant for deep lung penetration. - Conversely, drug powder showed deposition from stage 0 (particles more than $9.0 \mu\text{m}$) to stage 3 (particles between $3.4\text{-}4.6 \mu\text{m}$), which is relevant for deposition in the bronchial and laryngeal areas of the pulmonary tract.	[16]
9	Salbutamol sulfate	Alginic acid sodium salt from brown algae	In vitro aerodynamic test uses a next-generation impactor and a medium resistance single-	- Due to the high porosity of the aerogels, the aerodynamic diameter obtained for the particles was ca. 6-fold lower than the aerogel particle size and in the respirable range. - The emitted dose as the powder was	[15]

			<p>dose DPI. The capsules size 3 were manually filled with 8.0 ± 0.2 mg of powder, and the vacuum pump was activated at a flow of 60 L min^{-1} for 4.0 s. Before use, the seven collection stages of the impactor were coated with a 1 % (w/v) solution of glycerin in methanol and then allowed to dry.</p>	<p>close to 100%, indicating the aerogel particles' good flowability with reduced particle cohesion forces.</p> <ul style="list-style-type: none"> - The FPF values of the aerogels were close to 50 %, which means better performance than other inkjet-printed (5-23 %) particles and some SS-commercial formulations. - The SS deposition profile showed in the first stage of the impactor (36.7 %), and the deposited drug contents gradually decreased from stage 1 to 7.
10	Budesonide	Chitosan-gelatin	<p>Using a twin impinger. The 25-mg formulation loaded into an HPMC stick-free capsule was then installed in a Rotahaler® device containing 7 and 30 ml of collecting solvent (acetonitrile/ buffer) in stages 1 and 2, respectively. The system was vacuumed to produce air streams of 60 l/min for 5 s. The liquid in stages 1 and 2 was collected, diluted to 100 mL, and measured by UV spectrophotometry at 244 nm. Formulations were also subjected to Anderson cascade impactor (ACI) to determine the MMAD and GSD.</p>	<p>Pulmonary scintigraphy is a noninvasive method for visualizing deposition patterns and quantifying the amount of drug deposited and the concept of proof of bioavailability. BUD was radiolabeled with ^{99m}Tc by physical adsorption of radioactivity, then blended with inhalable lactose and filled in a size 3 capsule.</p> <ul style="list-style-type: none"> - Scintigraphic measurement after DPI inhalation—The radioactivity was obtained from RMC and was measured that the maximum respirable fraction obtained from radiolabeled BUD formulation was 22.16%, with a standard deviation of 4.31.
11	Rifampicin (RIF) and Rifabutin	Chitosan	<p>In vitro lung deposition of drug-loaded</p>	<ul style="list-style-type: none"> - A significant portion of the emitted dose was found deposited on the pre-separator stage (oral cavity). It is due

(RFB)	<p>microparticles, plain drug, and microparticles with lactose blends was evaluated on an Andersen Cascade Impactor (ACI) at a flow rate of 28.3 L/min using a Lupihaler device. Acceptable particle dose (FPD), fine particle fraction (FPF), mass median aerodynamic diameter (MMAD), and geometric standard deviation (GSD) were calculated as per USP using the CITDAS software application.</p>	<p>to the large particle size of the drug crystals, rod-shaped morphology of RIF, and agglomerated nature of RFB as observed in SEM images.</p> <p>- No significant differences were observed among the two batches of RIF-loaded microparticles concerning MMAD, GSD, and FPF. However, the values of MMAD and GSD near 5 μm and 1.2, respectively, indicate a monodisperse DPI system suitable for deep lung delivery.</p> <p>- RFB-loaded microparticles were similar to RIF-loaded microparticles. However, RFB-loaded microparticles showed better deposition in the later stages of the ACI, indicating a greater FPF.</p> <p>- RFB microparticles appear smooth and have a corrugated surface compared to RIF microparticles, which exhibited a rough surface.</p>
-------	--	---

Table 6: Lung Localization of Microparticles

No	Drug	Polymer	Method	Main Parameter	References
1	Paclitaxel	The sodium salt of alginic acid (Na-Alg) and hydroxypropyl methylcellulose (HPMC)	Anzatax, Free-PTX, and PTX-ALG-MPs were administered i.v. and endotracheally, and paclitaxel amount in lung tissue was determined at 0.5, 6, and 24 h after administration. Rats were killed, and the lungs were rapidly excised, weighed, frozen, and stored at -70 °C until analyzed.	- The amount of paclitaxel per gram of lung tissue after 0.5, 6 and 24 h was 19.1 ± 2.4, 2.7 ± 0.55 and 0.35 ± 0.13 μg for Free-PTX and 28.3 ± 0.4, 3.8 ± 0.5 and 0.35 ± 0.08 μg for PTX-ALGMPs. Lung tissue AUC for Free-PTX and PTX-ALG-MPs was 87.2 ± 2.4 and 124.8 ± 15.5 μg.h/ml. - Statistical analysis showed that paclitaxel amount in lung tissue 0.5 h after endotracheal delivery of Free-PTX and PTX-ALG-MPs was significantly higher than i.v administration due to local delivery of powders to the lung.	[8]
2	Isoniazid (INH)	Sodium alginate, Ispaghula husk and ^{99m} Tc-Technetium (^{99m} Tc).	Using three Wistar rats weighing about 300–350 g. The microparticles were administered orally, a dose of 37 mBq, after overnight fasting for 8–10 h. The animals were	- The gamma image was recorded by injecting the ^{99m} Tc via i.v. Route. High levels of ^{99m} Tc were detected in the lung, liver, and spleen immediately after injection. - During the gamma scintigraphy study, the presence of microparticles could be marked in	[45]

			<p>carried out normal activities but were not allowed to take any food or water until the formulation had emptied the stomach. The scintigraphic examination was done at 1, 4, and 12 h to assess the mobilization of the microparticles in the GIT. Images were recorded for a preset time of 5 min/view with a 15% window centered on including the 140 keV photopeak of ^{99m}Tc.</p>	<p>the intestinal lumen 1 h after the oral administration. Microparticles could also be detected in the intestine after 12 h. However, the percent radioactivity had significantly decreased ($t_{1/2}$ of ^{99m}Tc $\frac{1}{4}$ 4–5 h). Due to negligible radioactivity, microparticles in the GIT could not be assessed after 12 h of administration.</p> <p>- The optimized microparticles based on design software exhibited 83.43% drug entrapment and 51.53 μm particle size with 97.80% and 96.37% validity, respectively.</p>	
3	Lipopolysaccharide (LPS) from <i>K. pneumonia</i>	Sodium alginate	<p>The in vivo efficacy evaluation of free LPS and encapsulated LPS was carried out in Swiss albino mice. Groups of six mice were administered 100 μg free LPS, and LPS encapsulated microparticles (2 mg microparticles equivalent to 100 mg LPS) via intramuscular, intratracheal, and intranasal routes.</p>	<p>- The control group mice did not show any antibody titer against <i>K. pneumonia</i> LPS. In the case of the mice immunized with free and encapsulated LPS, variable PHA titers were observed, thus indicating that the LPS antigen is presently capable of inducing an immunological response.</p> <p>- Comparison of PHA titers of mice immunized with free LPS with those immunized with LPS encapsulated microparticles revealed a better antibody response irrespective of the route of administration. Maximum antibody response was observed in mice immunized with LPS encapsulated microparticles by intra-tracheal, intranasal, and intramuscular routes. The free LPS vaccine, on the contrary, has evoked very low PHA titers.</p>	[46]
4	Isoniazid	Sodium alginate	<p>Nine Wistar Rats (300–350 g; 15–20 weeks old) were used, each treated and untreated animal group. The microspheres were administered 2 mg/ml after overnight fasting for 8–10 h. Animals were given free access</p>	<p>- The i.v.-route administers the passage of ^{99m}Tc. Radioactivity was recorded in the thoracic and upper abdominal region and the tail region. High levels of ^{99m}Tc were detected in the lung, liver, and spleen immediately after injection.</p> <p>- Microspheres could be marked in the intestinal lumen 4 h post-oral administration. It showed the</p>	[47]

			<p>to water, but the food was restored 1–2 h after dosing. The animals' examination was done at 4 and 24 h to assess the mobilization of the microspheres in the GIT. Images were recorded for a preset 5 min/view, including the 140 keV photopeak of ^{99m}Tc.</p>	<p>contamination of the windpipe in one of the animals during oral administration. Microspheres could also be detected in the intestine after 24 h although the percent radioactivity had significantly decreased ($t_{1/2}$ of ^{99m}Tc = 4–5 h).</p> <ul style="list-style-type: none"> - The presence of microspheres in the GIT could not be assessed after 24 h of administration due to negligible radioactivity.
5	Rifampicin (RIF) and Isoniazid (INH)	Chitosan-Guar Gum	Spray-drying, ionotropic gelation	<ul style="list-style-type: none"> - All optimized formulations showed controlled and sustained drug release for a more extended period. - The optimized formulations also showed lower cytotoxicity and enhanced lung uptake of drugs. - Formulations also resulted in an almost 5-fold reduction in the number of bacilli in the lungs compared to free drugs.
6	Isoniazid (INH) and Rifabutin (RFB)	Carrageenan	<p>HPMC size 3 capsules were filled with 30 mg of CRG/ INH/RFB microparticles. The content of capsules loaded using the high resistance RS01® inhaler. The device was connected to the Andersen cascade impactor (ACI), operating at 60 L/min. It was activated for 4 s using the appropriate adaptor kit for the 60 L/min air flow rate test. Cut-offs of the stages (-1 to 6) at the airflow rates adopted. The impactor plates were coated with a solution of Tween 20® in ethanol 1% (w/v). The drugs were recovered with a water/ acetonitrile mixture (50/50, v/v) and quantified by HPLC. The recovery ranged</p>	<ul style="list-style-type: none"> - CRG/INH/RFB microparticles efficiently associated the model drugs, which antibacterial effect was not affected antibacterial effect. - The powder aerosolization performance was efficient, with emitted doses of 91% and MMAD of 3.3–3.9 μm, for RFB and INH, indicating a strong possibility of co-deposition of drugs in the deep lung region.

between 77 and 91% in all the experiments.

Table 7: Histopathological of Microparticles

No	Drug	Polymer	Method	Main Parameter	References
1	Ropinirole hydrochloride	Low viscosity sodium alginate	Using an isolated nasal sheep mucosa	<ul style="list-style-type: none"> - The size of microparticles had a narrow range (between 2.35 ± 0.10 and $2.58 \pm 0.06 \mu\text{m}$). - Histopathological of the microparticles (formulation A2) and drug-free microparticles did not show remarkable effects on the overall appearance of the animal's nasal mucosa, which is contrary to the positive control. No necrosis was detected. As shown, goblet cells, sero-mucinous glands, and ciliated cells were intact, with detection of only slight focal sloughing of the cells. 	[13]
2	Rifampicin (RIF) and isoniazid (INH)	Chitosan-based Nano embedded microparticles (CNPs), Mannan based Nano embedded microparticles (MNPs) and Guar gum-based Nano embedded microparticles (GNPs)	The isolated lung tissue was fixed in 5 mL of 10% neutral buffered formalin on female mice. Lungs were embedded, sectioned horizontally, stained with hematoxylin and eosin.	<ul style="list-style-type: none"> - Mannan batches show relatively higher pathological consequences evident by inflammatory cells and parenchyma degeneration. It could be related to the high burst release of ATDs, resulting in increased local drug concentration causing accidental cell death. - More substantial evidence of toxicity in mannan formulation is further related to preferential accumulation of mannan carrier in phagocytic cells due to the presence of mannose receptors predominantly found on their cell surface. - Other drug-loaded formulations show a thin layer of connective tissue and numerous capillaries lined with simple squamous epithelium without necrotizing granuloma. 	[48]
3	Budesonide	Sodium alginate-chitosa	The lung tissue of rats was fixed in 10% formalin for 24 h. The samples were then embedded in paraffin, cut into a 5 mm section,	<ul style="list-style-type: none"> - The obtained budesonide and commercial DPI particle sizes were 3.059 ± 0.03 and $1.521 \pm 0.04 \mu\text{m}$, respectively. - The formulated DPI showed higher entrapment efficiency 	[43]

			and stained with hematoxylin and eosin.	(87.16 ± 0.09%). - The MMAD of obtained budesonide and commercial DPI was 1.16 ± 0.01 and 5.04 ± 0.03 µm. - No signs of inflammation were observed in both samples treated animals. However, some basal membrane congestion was rarely observed in formulated DPI due to the installation procedure, which can be reversed by the anionic nature of the engineered particles.
4	Doxorubicin	Chitosan, BSA (fraction V, 99%), and Sodium alginate	Histology studies: lung specimens were fixed with formalin for at least 24 h, embedded in paraffin, sectioned, stained with hematoxylin and eosin.	- The H&E-stained tissue sections also showed that only a few small nodules existed in the lungs of mice treated with DOX-loaded capsules; in contrast, the mice treated with saline showed many melanomas, and metastasis nodules occupied a significant number of pulmonary parenchyma. [36]
5	Lovastatin (LS)	Sodium alginate (AG) powder and chitosan (CS) powder	On the 29th day, 40 adult Swiss mice were randomly divided into 4 groups, with 10 animals per group were injected with ketamine at a dose of 30mg/kg, and their kidneys and livers were excised, weighed, and examined macroscopically. Therefore, the livers and kidneys were preserved in 10% buffered formalin for histopathological study.	- The ACL nanoparticles containing a high LS content during the initial phase of the test period released less LS when compared with the ACL nanoparticles having a low LS concentration, where the release of LS from the ACL particles was higher. This drug release pattern occurred at all tested pH values, including 7.5, 6.5, 4.5, and 2. - Image of H&E-stained sections showing the glomerular and renal vein with edema exudate and a clear Bowman cavity with a normal kidney basement membrane. The vascularity of the cells was normal with relatively healthy tubular epithelial cells. The scale bar is 100 µm. [49]
6	Vancomycin hydrochloride	Sodium alginate and chitosan	Histological analysis was prepared in 4% phosphate-buffered paraformaldehyde and then washed overnight in water, dehydrated	- For more than 14 days, microspheres formulations showed no severe signs such as epithelial necrosis. The sloughing of epithelial cells was detected in histological studies. [34]

			through alcohols, cleared in xylene, and embedded in paraffin wax. The cut sections (5 µm in thickness) were stained with hematoxylin and eosin (H&E) and observed by microscope.	
7	Lipopolysaccharide (LPS) from <i>K. pneumoniae</i>	Sodium alginate	For histopathological evaluation, lung tissue was preserved in a 10% v/v aqueous formaldehyde solution. The excised lung tissues were dehydrated in ascending series of ethanol (70-100 %), embedded in paraffin wax, sectioned, and stained with hematoxylin-eosin. The severity of the pathological lesions was assessed on a semi-quantitative scale of 0-4, and a total score indicative of the overall severity was determined by adding the individual scores.	- Vaccinated animals showed significantly low severity scores (P-value < 0.05) compared to control animals, except for the animals that received encapsulated vaccines, which showed comparatively high lesion scores. - There is no edema or congestion in these animals, as seen in the untreated control group. Such infiltration of cells may be attributed to the particulate nature of the microparticles, which has caused a mild reaction and is a commonly reported observation on the administration of particulate delivery systems. - The LPS encapsulated microparticles exhibit greater efficacy when administered by the intra-tracheal route than the free LPS vaccine. The mice immunized with LPS encapsulated microparticles showed more significant PHA titers and revealed complete elimination of <i>K. pneumoniae</i> from lungs. [46]
8	Budesonide	Chitosan	The right lobes of mice and rats (which were not lavaged) were excised, fixed with 10 % formalin for 48 h, embedded in paraffin after alcohol gradient treatment, and then sliced into 5 µm thin sections for H&E staining. The inflammatory cell infiltrate was analyzed	- No statistical difference in the histology, inflammation cells, and IL-4 mRNA expression was found, indicating the chitosan microparticle itself did not affect asthma mice. - The significantly enhanced sustained therapeutic effect of chitosan swellable microparticles was demonstrated in allergic asthma models in mice and rats. After single treatment with SM50 and SM200, a time-dependent [50]

by light microscopy at a magnification of 100x. Briefly, the inflammation score was designated as none (score, 0), mild (score, 1-2), moderate inflammation (score, 3-4), or severe inflammation (score, 5-6). The final score was calculated by the addition of both peribronchial and perivascular inflammation.

therapeutic impact was investigated to test whether prolonged therapeutic efficacy can be achieved as a reflection of in vitro sustained release. - Both inflammatory cells and IL-4 and IL-5 levels in BALF showed delivery of SM200 and SM50, which had a sustained drug release for 12 h, had a longer therapeutic effect than budesonide physical mixture alone. - SM200 showed significant therapeutic efficacy up to 18 h.

3. Conclusions

This paper provides a comprehensive review of the current researches of various polymers in drug and protein delivery, particularly for inhalation in DPI dosage forms. Applications of polymers in these researches have a promising future. The characterization and testing of the polymer include stability, drug deposition to its histopathological. This review highlights the recent advances in polymers because of their convenience, biodegradability, and nontoxicity, and it is applied to various drug-delivery technologies. Thus, researchers need to update the advances in polymer-based drug delivery systems, and this review is a source of guidance for future research.

Acknowledgments

The authors thank the Faculty of Pharmacy and Universitas Airlangga for supporting this work.

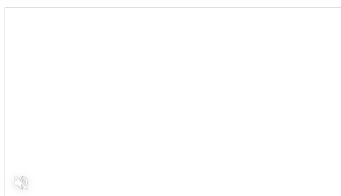
References

- [1] Bagherisadeghi G, Larhrib EH, Chrystyn H. Real life dose emission characterization using COPD patient inhalation profiles when they inhaled using a fixed dose combination (FDC) of the medium strength Symbicort® Turbuhaler®. *Int. J. Pharm.* 2017;522(1-2):137–46. <https://doi.org/10.1016/j.ijpharm.2017.02.057>.
- [2] Barrons R, Pegram A, Borries A. Inhaler Device Selection: Special Considerations in Elderly Patients with Chronic Obstructive Pulmonary Disease. *Am J Health-Syst Pharm.* 2011;68:1221-32. <https://doi.org/10.2146/ajhp100452>.
- [3] Sham JOH, Zhang Y, Finlay WH, Roa WH, Löbenberg R. Formulation and characterization of spray-dried powders containing nanoparticles for aerosol delivery to the lung. *Int J Pharm.* 2004;269(2):457–67. <https://doi.org/10.1016/j.ijpharm.2003.09.041>.
- [4] Ely L, Roa W, Finlay WH, Löbenberg R. Effervescent dry powder for respiratory drug delivery. *Eur J Pharm Biopharm.* 2007;65(3):346–53. <https://doi.org/10.1016/j.ejpb.2006.10.021>.
- [5] Labiris NR, Dolovich MB. Pulmonary Drug Delivery. Part I: Physiological Factors Affecting the Effectiveness of Inhaled Drugs. *R J Clin Pharmacol.* 2003;56:588-99. <https://doi.org/10.1046/j.1365-2125.2003.01892>.
- [6] Torchilin VP. *Nanoparticulates as Drug Carriers*. London: Imperial College Press, 2006.
- [7] Dolovich M. New Propellant-Free Technologies under Investigation. *J Aerosol Med.* 1999;12(s1):9-17. https://doi.org/10.1089/jam.1999.12.suppl_1.s-9.
- [8] Alipour S, Montaseri H, Khalili A, Tafaghodi M. Non-Invasive Endotracheal Delivery of Paclitaxel-Loaded Alginate Microparticles. *J Chemotherapy.* 2016;28(5): 411–6. <https://doi.org/10.1080/1120009x.2015.1105624>.
- [9] Möbus K, Siepman J, Bodmeier R. Zinc–Alginate Microparticles for Controlled Pulmonary Delivery of Proteins Prepared by Spray-Drying. *Eur J Pharm Biopharm.* 2012;81(1):121–30. <https://doi.org/10.1016/j.ejpb.2012.01.018>.
- [10] Athamneh T, Amin A, Benke E, Ambrus R, Leopold CS, Gurikov P, et al. Alginate and Hybrid Alginate-Hyaluronic Acid Aerogel Microspheres as Potential Carrier for Pulmonary Drug Delivery. *J Supercrit Fluids.* 2019;150:49-55. <https://doi.org/10.1016/j.supflu.2019.04.013>.
- [11] Yas A. Preparation and Characterization of In Situ Cross-Linking Alginate/Polyethylene Glycol 6000 Blend Microparticles for Controlling

- Salbutamol Sulphate Pulmonary Delivery. *Int J Pharm. Pharm. Sci.* 2013;5(4):728-33. <https://innovareacademics.in/journal/ijpps/Vol5Ssuppl4/8195.pdf>.
- [12] Hariyadi DM, Hendradi E. Effect of Polymer Concentration on Micromeritics, Kinetics, and Activity of Ciprofloxacin HCl-Alginate Microspheres. *Asian J Pharm.* 2019;13(4):349-55. <http://dx.doi.org/10.22377/ajp.v13i04.3408>.
- [13] Hussein N, Omer H, Ismael A, Albed Alhnan M, Elhissi A, Ahmed W. Spray-Dried Alginate Microparticles for Potential Intranasal Delivery of Ropinirole Hydrochloride: Development, Characterization and Histopathological Evaluation. *Pharm Dev Technol.* 2019;1–36. <https://doi.org/10.1080/10837450.2019.1567762>.
- [14] Islan GA, Bosio VE, Castro GR. Alginate Lyase and Ciprofloxacin Co-Immobilization on Biopolymeric Microspheres for Cystic Fibrosis Treatment. *Macromol Biosci.* 2013;13(9):1238–48. <https://doi.org/10.1002/mabi.201300134>.
- [15] López-Iglesias C, Casielles AM, Altay A, Bettini R, Alvarez-Lorenzo C, García-González CA. From the Printer to the Lungs: Inkjet-Printed Aerogel Particles for Pulmonary Delivery. *Chem Eng J.* 2018, <https://doi.org/10.1016/j.cej.2018.09.159>.
- [16] Mahmoud AA, Elkasabgy NA, Abdelkhalek AA. Design and Characterization of Emulsified Spray Dried Alginate Microparticles as A Carrier for the Dually Acting Drug Roflumilast. *Eur J Pharm Sci.* 2018;122:64–76. <https://doi.org/10.1016/j.ejps.2018.06.015>.
- [17] Ainali NM, Xanthopoulou E, Michailidou G, Zamboulis A, Bikiaris DN. Microencapsulation of Fluticasone Propionate and Salmeterol Xinafoate in Modified Chitosan Microparticles for Release Optimization. *Molecules.* 2020;25:3888. <https://doi.org/10.3390/molecules25173888>.
- [18] Cunha L, Rodrigues S, da Costa AMR, Faleiro L, Buttini F, Grenha A. (2019). *Inhalable Chitosan Microparticles for Simultaneous Delivery of Isoniazid And Rifabutin in Lung Tuberculosis Treatment, Drug Development, and Industrial Pharmacy*, <https://doi.org/10.1080/03639045.2019.1608231>.
- [19] Debnath, S. K., Saisivam, S., Debanth, M., Omri, A. (2018). *Development and Evaluation of Chitosan Nanoparticles Based Dry Powder Inhalation Formulations of Prothionamide*. *PLoS ONE*, 13(1): e0190976. <https://doi.org/10.1371/journal.pone.0190976>.
- [20] El-Sherbiny, I. M., & Smyth, H. D. C. (2010). *Biodegradable Nano-Micro Carrier Systems for Sustained Pulmonary Drug Delivery: (I) Self-Assembled Nanoparticles Encapsulated in Respirable/Swellable Semi-IPN Microspheres*. *Int J Pharmaceutics*, 395, 132–141. <https://doi.org/10.1016/j.ijpharm.2010.05.032>.
- [21] Kamble, M. S., Mane, O. R., Borwandkar, V. G., Mane, S. S., & Chaudhari, P. D. (2012). *Formulation and Evaluation of Clindamycin HCl – Chitosan Microspheres for Dry Powder Inhaler Formulation*. *Drug Invention Today*, 4(10), 527-530.
- [22] Merchant, Z., Taylor, K. M. G., Stapleton, P., Razak, S. A. R., Kunda, N., Alfagih, I., Sheik, K., Saleem, I., Y., & Somavarapu, S. (2014). *Engineering Hydrophobically Modified Chitosan for Enhancing the Dispersion of Respirable Microparticles of Levofloxacin*. *Eur J Pharmaceutics and Biopharmaceutics*, 1-14. <https://doi.org/10.1016/j.ejpb.2014.09.005>.
- [23] Pai, R. V., Jain, R. R., Bannaliker, A. S., & Menon, M. D. (2016). *Development and Evaluation of Chitosan Microparticles Based Dry Powder Inhalation Formulations of Rifampicin and Rifabutin*, *J Aerosol Med Pulmo Drug Deliv*, 28, 1–17. <https://doi.org/10.1089/jamp.2014.1187>.
- [24] Rawal, T., Parmar, R., Tyagi, R. K., & Butani, S. (2017). *Rifampicin Loaded Chitosan Nanoparticle Dry Powder Presents: An Improved Therapeutic Approach for Alveolar Tuberculosis, Colloids, and Surfaces B: Biointerfaces*. S0927-7765(17)30162-5. <https://doi.org/10.1016/j.colsurfb.2017.03.044>.
- [25] Shen, Y. B., Zhe, D., Tang, C., Guan, Y. X., Yao, S. J. (2016). *Formulation of Insulin-Loaded N-Trimethyl Chitosan Microparticles with Improved Efficacy for Inhalation by Supercritical Fluid Assisted Atomization*. *Int J Pharmaceutics*, S0378-5173(16)30262-9. <https://doi.org/10.1016/j.ijpharm.2016.03.053>.
- [26] Devi, N., & Maji, T. K. (2010). *Microencapsulation of Isoniazid in Genipin-Crosslinked Gelatin-A-κ-Carrageenan Polyelectrolyte Complex*. *Drug Development and*

- Industrial Pharmacy*, 36(1), 56–63. <https://doi.org/10.3109/03639040903061355>.
- [27] Hariyadi, D. M., Hendradi, E., & Sharon, N. (2019). *Development of Carrageenan Polymer for Encapsulation of Ciprofloxacin HCl: In Vitro Characterization*. *Int J Drug Deliv Tech*, 9(1); 89-93. <https://doi.org/10.25258/ijddt.9.1.14>.
- [28] Rodrigues, S., Cunha, L., Rico, J., Rosa da Costa, A.M., Almeida, A.J., Faleiro, M.L., Buttini, F., & Grenha, A. (2020). *Carrageenan from red algae: an application in the development of inhalable tuberculosis therapy targeting the macrophages*. *Drug Delivery and Translational Research*, 10:1675–168. <https://doi.org/10.1007/s13346-020-00799-0>.
- [29] Hill, M., Matthew T., Emer A. S., John G. H., J. Stuart E., Clifford C. T., Christopher J. S., & Marie E. M. (2019). *Alginate/Chitosan Particle-Based Drug Delivery Systems for Pulmonary Applications*, *Pharmaceutics*, 11(8), Article number: 379 p. 1-12. <https://doi.org/10.3390/pharmaceutics11080379>.
- [30] Abdelghany, S., Alkhaldeh, M., & Alkhatib, H. S. (2017). *Carrageenan-Stabilized Chitosan Alginate Nanoparticles Loaded with Ethionamide for the Treatment of Tuberculosis*. *J Drug Delivery*, 39, 442-449. <https://doi.org/10.1016/j.jddst.2017.04.034>.
- [31] Deacon, J., Abdelghany, S. M., Quinn, D. J., Schmid, D., Megaw, J., Donnelly, R. F., Scott, C. J. (2015). *Antimicrobial Efficacy of Tobramycin Polymeric Nanoparticles for Pseudomonas aeruginosa Infections in Cystic Fibrosis: Formulation, Characterisation, and Functionalisation with Dornase Alfa (DNase)*. *Journal of Controlled Release*, 198, 55–61. <https://doi.org/10.1016/j.jconrel.2014.11.022>.
- [32] Elmowafy, E., & Soliman, M. E. (2019). *Losartan-Chitosan/Dextran Sulfate Microplex as A Carrier to Lung Therapeutics: Dry Powder Inhalation, Aerodynamic Profile, and Pulmonary Tolerability*. *Int J Biological Macromolecules*, 136, 220–229. <https://doi.org/10.1016/j.ijbiomac.2019.06.058>.
- [33] Mali, A. J., Pawar, A. P., & Bothiraja, C. (2014). *Improved Lung Delivery of Budesonide from Biopolymer Based Dry Powder Inhaler Through Natural Inhalation of Rat*. *Materials Technology*, 29(6), 350–357. <https://doi.org/10.1179/1753555714y.0000000163>.
- [34] Mao, Y., Ming, Z., Yongbiao, G., & Jiang F. (2016). *Novel Alginate-Chitosan Composite Microspheres for Implant Delivery of Vancomycin and In Vivo Evaluation*, *Chem Biol Drug Des*, 88(3), 434-440. <https://doi.org/10.1111/cbdd.12771>.
- [35] Leena, M. M., Antoniraja, M. G., Mosesa, J. A., & Anandharamakrishnana, C. (2020). *Three Fluid Nozzle Spray Drying for Co-Encapsulation and Controlled Release of Curcumin and Resveratrol*. *J Drug Deliv Sci-Tech*, 57, 101678. <https://doi.org/10.1016/j.jddst.2020.101678>.
- [36] Shen, H., Shi, H., Xie, M., Ma, K., Li, B., Shen, S., Jin, Y. (2013). *Biodegradable Chitosan/Alginate BSA-Gel-Capsules for pH-Controlled Loading and Release of Doxorubicin and Treatment of Pulmonary Melanoma*. *Journal of Materials Chemistry B*, 1(32), 3906. <https://doi.org/10.1039/c3tb20330a>.
- [37] Jaya, S., Durance, T. D., & Wang, R. (2008). *Effect of alginate-pectin composition on drug release characteristics of microcapsules*. *Journal of Microencapsulation*, 26(2), 143–153. <https://doi.org/10.1080/02652040802211345>.
- [38] Alipour, S., Montaseri, H., & Tafaghodi, M. (2010). *Preparation and Characterization of Biodegradable Paclitaxel Loaded Alginate Microparticles for Pulmonary Delivery*. *Colloids and Surfaces B: Biointerfaces*, 81(2), 521–529. <https://doi.org/10.1016/j.colsurfb.2010.07.050>.
- [39] Manca, M. L., Valenti, D., Sales, O. D., Nacher, A., Fadda, A. M., & Manconi, M. (2014). *Fabrication of Polyelectrolyte Multilayered Vesicles as Inhalable Dry Powder for Lung Administration of Rifampicin*. *International Journal of Pharmaceutics*, 472(1-2), 102–109. <https://doi.org/10.1016/j.ijpharm.2014.06.009>.
- [40] Rodrigues, S., Cordeiro, C., Seijo, B., Remuñán-López, C., & Grenha, A. (2015). *Hybrid Nanosystems Based on Natural Polymers as Protein Carriers for Respiratory Delivery: Stability and Toxicological Evaluation*. *Carbohydrate Polymers*, 123, 369–380. <https://doi.org/10.1016/j.carbpol.2015.01.048>.
- [41] Sivadas, N., O'Rourke, D., Tobin, A., Buckley, V., Ramtoola, Z., Kelly, J. G., Cryan, S.-A. (2008). *A Comparative Study of A Range of Polymeric Microspheres as Potential Carriers for the Inhalation of Proteins*. *International Journal of Pharmaceutics*, 358(1-2), 159–167. <https://doi.org/10.1016/j.ijpharm.2008.03.024>.

- [42] Sivadas, N., & Cryan, S.-A. (2011). *Inhalable, Bioresponsive Microparticles for Targeted Drug Delivery in the Lungs*. *Journal of Pharmacy and Pharmacology*, 63(3), 369–375. <https://doi.org/10.1111/j.2042-7158.2010.01234.x>.
- [43] Mali, A. J., Pawar, A. P., & Purohit, R. N. (2014). *Development of Budesonide Loaded Biopolymer Based Dry Powder Inhaler: Optimization, In-Vitro Deposition, and Cytotoxicity Study*. *J Pharm*, 793571, 12pages. <https://doi.org/10.1155/2014/795371>.
- [44] Naikwade, S. R., Bajaj, A. N., Gurav, P., Gatne, M. M., & Soni, P. S. (2009). *Development of Budesonide Microparticles Using Spray-Drying Technology for Pulmonary Administration: Design, Characterization, In Vitro Evaluation, and In Vivo Efficacy Study*. *AAPS PharmSciTech*, 10(3). <https://doi.org/10.1208/s12249-009-9290-6>.
- [45] Maurya, D. P., Sultana, Y., Aqil, M., Kumar, D., Chuttani, K., Ali, A., & Mishra, A. K. (2011). *Formulation and Optimization of Alkaline Extracted Ispaghula Husk Microparticles of Isoniazid–In Vitro and In Vivo Assessment*. *Journal of Microencapsulation*, 28(6), 472–482. <https://doi.org/10.3109/02652048.2011.580861>.
- [46] Jain, R. R., Mehta, M. R., Bannaliker, A. R., & Menon, M. D. (2015). *Alginate Microparticles Loaded with Lipopolysaccharide Subunit Antigen for Mucosal Vaccination against Klebsiella pneumoniae*. *Biologicals*, 43(3), 195–201. <https://doi.org/10.1016/j.biologicals.2015.02.001>.
- [47] Rastogi, R., Sultana, Y., Aqil, M., Ali, A., Kumar, S., Chuttani, K., & Mishra, A. (2007). *Alginate Microspheres of Isoniazid for Oral Sustained Drug Delivery*. *International Journal of Pharmaceutics*, 334(1-2), 71–77. <https://doi.org/10.1016/j.ijpharm.2006.10.024>.
- [48] Goyal, A. K., Garg, T., Rath, G., Gupta, U. D., & Gupta, P. (2015). *Development and Characterization of Nanoembedded Microparticles for Pulmonary Delivery of Antitubercular Drugs against Experimental Tuberculosis*. *Molecular Pharmaceutics*, 12(11), 3839–3850. <https://doi.org/10.1021/acs.molpharmaceut.5b00016>.
- [49] Thai, H., Thuy Nguyen, C., Thi Thach, L., Thi Tran, M., Duc Mai, H., Thi Thu Nguyen, T., Van Le, Q. (2020). *Characterization of Chitosan/Alginate/Lovastatin Nanoparticles and Investigation of Their Toxic Effects In Vitro and In Vivo*. *Scientific Reports*, 10(1). <https://doi.org/10.1038/s41598-020-57666-8>.
- [50] Zhang, L., Yang, L., Zhang, X., Jiaqi, L., Fan, L., Beck-Broichsitter, M., Zhang, X., Muenster, U., Wang, X., Zhao, J., Zhang, Y., & Mao, S. (2017). *Sustained Therapeutic Efficacy of Budesonide-Loaded Chitosan Swellable Microparticles After Lung Delivery: Influence of In Vitro Release, Treatment Interval, and Dose*. *J Controlled Release*, S0168-3659(18)30315-8. <https://doi.org/10.1016/j.jconrel.2018.05.031>.



Egyptian Journal of Chemistry

COUNTRY

Egypt

Universities and research institutions in Egypt

Media Ranking in Egypt

SUBJECT AREA AND CATEGORY

 Chemistry
 Chemistry (miscellaneous)

PUBLISHER

 NIDOC
 (Nat.Inform.Document.Centre)

H-INDEX

18

PUBLICATION TYPE

Journals

ISSN

04492285

COVERAGE

2004-2021

INFORMATION

[Homepage](#)
[How to publish in this journal](#)
mrh_mahran@yahoo.com

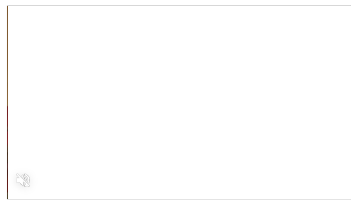
Glass-lined Reactors

SCOPE

The Egyptian Journal of Chemistry, a multidisciplinary chemistry journal, is a peer reviewed international journal, a free access journal and edited by the Egyptian Chemical Society and published monthly by NIDOC . Manuscripts that truly define the aims of the journal include, the fields of analytical, inorganic, organic, physical chemistry, applied and materials chemistry as well as all other branches of chemistry and its sub-disciplines like pharmaceutical, textile, environmental chemistry, biochemistry, polymer chemistry, petroleum chemistry, and agricultural chemistry, etc.

Join the conversation about this journal

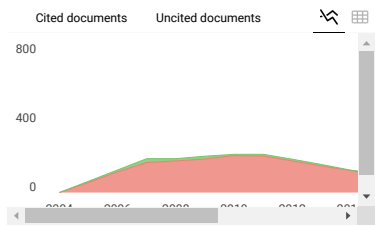
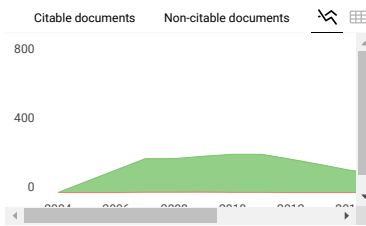
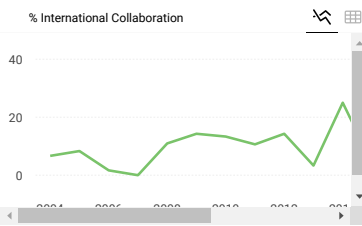
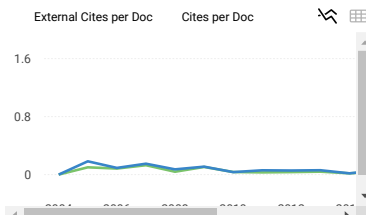
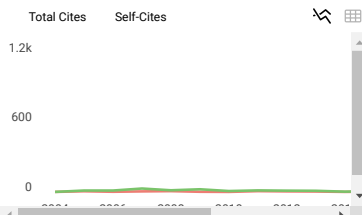
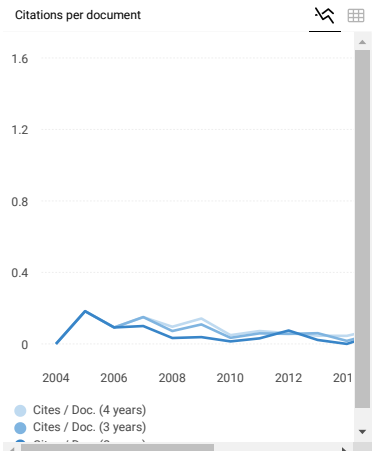
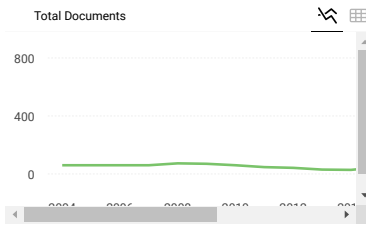
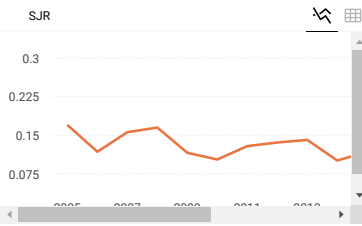
Glass-lined Reactors



FIND SIMILAR JOURNALS ?

options ⋮

- 1 **Arabian Journal of Chemistry**
SAU
45% similarity
- 2 **Journal of the Chemical Society of Pakistan**
PAK
44% similarity
- 3 **Asian Journal of Chemistry**
IND
43% similarity
- 4 **Research Journal of Chemistry and Environment**
IND
43% similarity
- 5 **Mediterranean Journal of Chemistry**
MAR
43% similarity



Egyptian Journal of Chemistry

Q3
Chemistry (miscellaneous)
best quartile

SJR 2021
0.23

powered by scimagojr.com

Show this widget in your own website

Just copy the code below and paste within your html code:

<a href="https://www.scimag

SCImago Graphica

Explore, visually communicate and make sense of data with our **new data visualization tool.**

